1   **Results from a Multi-Laboratory Ocean Metaproteomic Intercomparison:**

2   **Effects of LC-MS Acquisition and Data Analysis Procedures**

3   ***Participants of the Ocean Metaproteome Intercomparison Consortium:***

4   Mak A. Saito[*1], Jaclyn K. Saunders[1+], Matthew R. McIlvin[1], Erin M. Bertrand[2], John A. Breier[3],
5   Margaret Mars Brisbin[1], Sophie M. Colston[4], Jaimee R. Compton[4], Tim J. Griffin[5], W. Judson
6   Hervey[4], Robert L. Hettich[6], Pratik D. Jagtap[5], Michael Janech[7], Rod Johnson[8], Rick Keil[9], Hugo
7   Kleikamp[10], Dagmar Leary[4], Lennart Martens[17,18], J. Scott P. McCain[2,11], Eli Moore[12], Subina
8   Mehta[5], Dawn M. Moran[1], Jacqui Neibauer[7], Benjamin A. Neely[13], Michael V. Jakuba[1], Jim
9   Johnson[5], Megan Duffy[7], Gerhard J. Herndl[14], Richard Giannone[6], Ryan Mueller[15], Brook L.
10   Nunn[9], Martin Pabst[9], Samantha Peters[6], Andrew Rajczewski[5], Elden Rowland[2], Brian
11   Searle[16],Tim Van Den Bossche[17,18], Gary J. Vora[4], Jacob R. Waldbauer[19], Haiyan Zheng[20],
12   Zihao Zhao[14]
13
14   [1]Woods Hole Oceanographic Institution, Woods Hole, MA, USA
15   [2]Department of Biology, Dalhousie University, Halifax, NS, Canada
16   [3]The University of Texas Rio Grande Valley, Edinburg, TX
17   [4]Center for Bio/Molecular Science & Engineering, Naval Research Laboratory, Washington, DC, USA
18   [5]University of Minnesota at Minneapolis, Minneapolis, Minnesota, USA
19   [6]Oak Ridge National Laboratory, Oak Ridge, Tennessee, USA
20   [7]College of Charleston, Charleston, South Carolina, USA
21   [8]Bermuda Institute of Ocean Sciences, Bermuda
22   [9]University of Washington, Seattle, Washington, USA
23   [10]Department of Biotechnology, Delft University of Technology, Netherlands
24   [11]Department of Biology, Massachusetts Institute of Technology, Cambridge, MA, USA
25   [12] United States Geological Survey, USA
26   [13]National Institute of Standards and Technology, Charleston, South Carolina, USA
27   [14]University of Vienna, Dept. of Functional and Evolutionary Ecology, Austria
28   [15]Oregon State University, Corvallis, Oregon, USA
29   [16]Ohio State University, Columbus, Ohio, USA
30   [17]Department of Biomolecular Medicine, Faculty of Medicine and Health Sciences, Ghent University, 9000
31   Ghent, Belgium
32   [18]VIB – UGent Center for Medical Biotechnology, VIB, 9000 Ghent, Belgium
33   [19]Department of Geophysical Sciences, University of Chicago, Chicago, Illinois, USA
34   [20]Rutgers University, Piscataway, New Jersey, USA
35   [+]Present address: University of Georgia, Department of Marine Sciences
36   * corresponding author, msaito@whoi.edu

39   *Submitted to Biogeosciences 12/27/2023*

40   *Revision for Biogeosciences 7/3/2024*

42   **Abstract**

43   Metaproteomics is an increasingly popular methodology that provides information regarding the

44   metabolic functions of specific microbial taxa and has potential for contributing to ocean ecology

45   and biogeochemical studies. A blinded multi-laboratory intercomparison was conducted to

46   assess comparability and reproducibility of taxonomic and functional results and their sensitivity

47   to methodological variables. Euphotic zone samples from the Bermuda Atlantic Time-Series

48   Study in the North Atlantic Ocean collected by *in situ* pumps and the AUV *Clio* were distributed

49   with a paired metagenome, and one-dimensional liquid chromatographic data dependent

50   acquisition mass spectrometry analyses was stipulated. Analysis of mass spectra from seven

51   laboratories through a common bioinformatic pipeline identified a shared set of 1056 proteins

52   from 1395 shared peptides constituents. Quantitative analyses showed good reproducibility:

53   pairwise regressions of spectral counts between laboratories yielded R^2 values averaged 0.62

54   +/- 0.11, and a Sørensen similarity analysis of the top 1,000 proteins revealed 70-80% similarity

55   between laboratory groups. Taxonomic and functional assignments showed good coherence

56   between technical replicates and different laboratories. A bioinformatic intercomparison study,

57   involving 10 laboratories using 8 software packages successfully identified thousands of

58   peptides within the complex metaproteomic datasets, demonstrating the utility of these software

59   tools for ocean metaproteomic research. Lessons learned and potential improvements in

60   methods were described. Future efforts could examine reproducibility in deeper metaproteomes,

61   examine accuracy in targeted absolute quantitation analyses, and develop standards for data

62   output formats to improve data interoperability. Together, these results demonstrate the

63   reproducibility of metaproteomic analyses and their suitability for microbial oceanography

64   research including integration into global scale ocean surveys and ocean biogeochemical

65   models.

66

1. Introduction

Microorganisms within the oceans are major contributors to global biogeochemical cycles, influencing the cycling of carbon, nitrogen, phosphorus, sulfur, iron, cobalt and other elements (Falkowski et al., 2008; Moran et al., 2022; Worden et al., 2015). 'Omic methodologies can provide an expansive window into these communities, with genomic approaches characterizing the diversity and potential metabolisms, and transcriptomic and proteomic methods providing insights into expression and function of that potential. Similar to other 'omics approaches, proteomics is increasingly being applied to natural ocean environments and the diverse microbial communities within them. When proteomics is applied to such mixed communities, it is generally referred to as metaproteomics (Wilmes and Bond, 2006). Metaproteomic samples contain an extraordinary level of complexity relative to single organism proteomes (at least 1-2 orders of magnitude) due to the simultaneous presence of many different organisms in widely varying abundances (McCain and Bertrand, 2019). In particular, ocean metaproteome samples are significantly more complex than the human proteome, the latter of which is itself considered to be a highly complex sample (Saito et al., 2019). Proteomics (including metaproteomics) provides a perspective distinct from other 'omics methods: as a direct measurement of cellular functions it can be used to examine the diversity of ecosystem biogeochemical capabilities, to determine the extent of specific nutrient stressors by measurement of transporters or regulatory systems, to determine cellular resource allocation strategies in-situ, estimate biomass contributions from specific microbial groups, and even to estimate potential enzyme activity (Bender et al., 2018; Bergauer et al., 2018; Cohen et al., 2021; Fuchsman et al., 2019; Georges et al., 2014; Hawley et al., 2014; Held et al., 2021; Leary et al., 2014; McCain et al., 2022; Mikan et al., 2020; Moore et al., 2012; Morris et al., 2010; Saito et al., 2020; Sowell et al., 2009; Williams et al., 2012). The functional perspective that metaproteomics allows is often complementary to metagenomic and metatranscriptomic analyses and can provide biological

92   insights that are distinct from organisms studied in the laboratory (Kleiner et al., 2019).

93   Moreover, the measurement of microbial proteins in environmental samples has improved

94   greatly in recent years, due to the advancements in nanospray-liquid chromatography and high-

95   resolution mass spectrometry approaches (Mueller and Pan, 2013; Ram et al., 2005; McIlvin

96   and Saito, 2021).

97   With increasing interest in the measurement of proteins and their biogeochemical

98   functions within the oceans, the metaproteomic data is beginning to establish itself as a valuable

99   research and monitoring tool. However, given rapid changes in technology and methods, as well

100   as the overall youth of the metaproteomic field, demonstrating the reproducibility and

101   robustness of metaproteomic measurements to microbial ecology and oceanographic

102   communities is an important goal. This is particularly true as applications for metaproteomics

103   expand in research and monitoring of the changing ocean environment, for example in global

104   scale efforts such as the developing BioGeoSCAPES program (www.biogeoscapes.org;

105   (Tagliabue, 2023)), which aims to characterize the ocean metabolism and nutrient cycles on a

106   changing planet. As a result, there is a pressing need to assess inter-laboratory consistency,

107   and to understand the impacts of sampling, extraction, mass spectrometry, and bioinformatic

108   analyses on the biological inferences that can be drawn from the data.

109   There have been efforts to conduct intercomparisons of metaproteomic analyses in both

110   biomedical and environmental sample types in recent years that provide precedent for this

111   study. A recent community best practice effort in ocean metaproteomics data-sharing also

112   identified major challenges in ocean metaproteomics research, including sampling, extraction,

113   sample analysis, bioinformatics pipelines, and data sharing, and conducted a quantitative

114   assessment of sample complexity in ocean metaproteome samples (Saito et al., 2019). A

115   previous benchmark study, driven by the Metaproteomics Initiative (Van Den Bossche et al.,

116   2021), was the "Critical Assessment of Metaproteome Investigation study" (CAMPI) that

117   employed a laboratory-assembled microbiome and human fecal microbiome sample to

118   successfully demonstrate reproducibility of results between laboratories. CAMPI found

119   robustness in results across datasets, while also observing variability in peptide identifications

120   largely attributed to sample preparation. This observation was consistent with prior findings on

121   single organism samples that determined >70% of the variability was due to sample processing,

122   rather than chromatography and mass spectrometry (Piehowski et al., 2013). Finally, the

123   Proteomics Informatics Group (iPRG) from the Association of Biomolecular Resources Facilities

124   (ABRF) conducted a study examining the influence of informatics pipelines on metaproteomics

125   analyses that found consistency among research groups in taxonomic attributions (Jagtap et al.,

126   2023), and previous research has demonstrated the impact of database choices on final

127   functional annotations and biological implications (Timmins-Schiffman et al., 2017).

128   Here we describe the results from the first ocean metaproteomic intercomparison. In this

129   study, environmental ocean samples were collected from the euphotic zone of the North Atlantic

130   Ocean and partitioned into subsamples and distributed to an international group of laboratories

131   (Fig. 1). The study was designed to examine inter-laboratory consistency rather than maximal

132   capabilities, stipulating one-dimensional chromatographic analyses from each laboratory (with

133   optional deeper analysis). Users were invited to use their preferred extraction, analytical, and

134   bioinformatic procedures. The effort focused on the data dependent analysis (DDA) methods,

135   also known as global proteomics where the targets are unknown and hence there is a discovery

136   element to the approach. DDA is currently common in ocean and other environmental and

137   biomedical metaproteomics, and its spectral abundance units of relative quantitation have been

138   shown to be reproducible in metaproteomics (Kleiner et al., 2017; Pietilä et al., 2022). Blinded

139   results were submitted, compared and discussed at a virtual community workshop in September

140   of 2021. An additional bioinformatic pipeline comparison study was also conducted where

141   participants were provided metaproteomic raw data and associated metagenomic sequence

142   database files and were encouraged to use the bioinformatic pipeline of their choice.

143   **2. Methods**

144   *2.1 Sample Collection and Metadata*

145   Ocean metaproteome filter samples for the wet lab comparison (Figure 1) were collected

146   at the Bermuda Atlantic Time-series Study (31° 40'N 64 ° 10'W) on expedition BATS 348 on

147   June 16th, 2018, between 01:00 and 05:00 am local time. *In situ* (underwater) large volume

148   filtration was conducted using submersible pumps to produce replicate biomass samples at a

149   single depth in the water column for intercomparisons. All filter subsamples are matched for

150   location, time, and depth. To collect the samples, two horizontal McLane pumps were clamped

151   together (Figure 1c) and attached at the same depth (80 m) with two filter heads (Mini-MULVS

152   design) on each pump and a flow meter downstream of each filter head. This depth was chosen

153   to correspond to a depth with abundant chlorophyll and photosynthetic organisms. Each filter

154   head contained a 142 mm diameter 0.2 μm pore-size Supor (Pall Inc.) filter with an upstream

155   142 mm diameter 3.0 μm pore-size Supor (Figure 1b, d). Only the 0.2 – 3.0 μm size fraction

156   was used in this study. The pumps were set to run for 240 min at 3 L per min. Volume filtered

157   was measured by three gauges on each pump, one downstream of each pump head, and one

158   on the total outflow (Table S2). Individual pump head gauges summed to the total gauge for

159   pump 1 (within 1 L; 447 L and 446.2 L), but deviated by 89 L on pump 2 (478 L and 388.9 L).

160   Given that the total gauge is further downstream, we report the pump head gauges as being

161   more accurate.

162   The pump heads were removed from the McLane pumps immediately upon retrieval,

163   decanted of excess seawater by vacuum, placed in coolers with ice packs, and brought into a

164   fabricated clean room environment aboard the ship. The 0.2 μm pore-size filters were cut in

165 eight equivalent pieces and frozen at -80°C in 2 mL cryovials, creating 16 samples per pump

166 that were co-collected temporally and in very close proximity (<1 m) to each other for a total of

167 32 samples used in this study (Figure 1d). The 3.0 µm pore-size filters are not included in this

168 study but are archived for future efforts. The sample naming scheme associated with the

169 different pumps and pump heads is described in Table S2. Note that pump 1A and 1B samples

170 accidentally had two 3.0 µm filters superimposed above the 0.2 µm filter, and 1B had a small

171 puncture in it, although neither of these seemed to affect the biomass collected, presumably the

172 puncture occurred after sampling was completed.

173   Samples for the bioinformatic component were collected by the autonomous underwater

174 vehicle *Clio*. The vehicle and its sampling characteristics were used as previously described

175 (Breier et al., 2020; Cohen et al., 2023). Specifically, samples Ocean-8 and Ocean-11 were

176 also collected from the BATS station on R/V *Atlantic Explorer* expedition identifier AE1913 (also

177 described as BATS validation track BV55 32.75834º N 65.7374º W). The samples were

178 collected by autonomous underwater vehicle (AUV) *Clio* on June 19th 2019, dive Clio020, with

179 samples collected at 20 m (Ocean-11) and 120 m (Ocean-8) with 66.6 L and 92.6 L filtered,

180 respectively, used for this study. These depths were chosen to reflect the near surface (high-

181 light) and deep chlorophyll maximum (low-light) communities present in the stratified summer

182 conditions. These samples were analyzed by 1D DDA analysis using extraction and mass

183 spectrometry for laboratory 438 within their laboratory (Tables S5-S7). Sample metadata for

184 both arms of this intercomparison study and corresponding repository information is provided in

185 Table S3 and repository links are in the Data Availability Statement.

186 *2.2 Metagenomic Extraction, Sequencing, and Assembly*

187   A metagenomic (reference sequence) database was created for peptide to spectrum

188 matching (PSMs) for the metaproteomic studies using a 1/8th sample split from the exact

189   sample used in the intercomparison as described above. Samples were shipped on dry ice to

190   the Naval Research Laboratory in Washington D.C. (USA), where DNA was extracted and

191   sequenced. Preserved filters were cut into smaller pieces using a sterile blade and placed into a

192   PowerBead tube with a mixture of zirconium beads and lysis buffer (CD1) from the Dneasy

193   PowerSoil Pro kit (Qiagen, Hilden Germany). The bead tube with filter sample was heated at

194   65°C for 10 min then placed on a vortex adapter and vortexed at maximum speed for 10 min.

195   After sample homogenization/lysis, the bead tube was centrifuged at 16 k x g for 2 min. The

196   supernatant was transferred to a DNA LoBind tube and processed using the manufacturer's

197   recommendations. The purified DNA was further concentrated by adding 10 µL3 M NaCl and

198   100 µL cold 100% ethanol. The sample was incubated at -30°C for 1 hour, followed by

199   centrifugation at 16 k x g for 10 min. The supernatant was removed and precipitated DNA was

200   air-dried and resuspended in 10 mM Tris. DNA concentration was quantified with the Qubit

201   dsDNA High Sensitivity assay (Thermo Fisher Scientific, Waltham, MA, USA) and DNA quality

202   was assessed using the NanoDrop (ThermoFisher) and gel electrophoresis. Processing controls

203   included reagent only and blank filter samples.

204   Sequencing libraries were created from purified sample DNA using the IonExpress Plus

205   gDNA Fragment Library Preparation kit (Thermo Fisher) for a 200 bp library insert size. No

206   amplification of the library was required as determined by qPCR using the Ion Library TaqMan

207   Quantitation Kit. A starting library concentration of 100 pM was used in template generation and

208   chip loading with the Ion 540 Kit on the Ion Chef instrument prior to single-end sequencing on

209   the S5 benchtop sequencer.

210   Sequencing used a mix of Ion Torrent and Oxford Nanopore sequencing and resulting

211   sequencing reads were assembled using SPAdes v. 3.13.1 with Python v. 3.6.8. Following

212   metagenome assembly, contigs smaller than 500 bases were discarded. Open reading frame

213   (ORF) calling was performed on contigs 500 bps or longer using Prodigal v. 2.6.3 (Hyatt et al.,

214   2010) run with metagenomic settings as well as MetaGeneMark by submitting to the

215   MetaGeneMark server (http://exon.gatech.edu/meta_gmhmmp.cgi) using GeneMark.hmm

216   prokaryotic program v. 3.25 on August 11, 2019. ORFs called from both programs were

217   combined and made non-redundant using in-house Python scripts that utilize BioPython v. 1.73.

218   Non-redundant ORFs were annotated using the sequence alignment program DIAMOND (v 0.9.29)

219   with the NCBI nr database (downloaded 12/17/2019). ORFs were also annotated with InterProScan

220   (v 5.29) and with GhostKOALA (Kanehisa et al., 2016) (submitted to server 1/2/2020). Taxonomy

221   lineages were generated by using the best DIAMOND (Buchfink et al., 2015) hit and pulling lineage

222   information from NCBI Taxonomy database using BioPython v. 1.73

223   *2.3 Proteomic methodologies: Extraction, instrumentation, and bioinformatics*

224   Some basic protocol stipulations were provided to study participants regarding analytical

225   conditions to set a uniformity of experimental design. While users were encouraged to use the

226   extraction method of their preference, constraints on chromatography and mass spectrometry

227   conditions were set, limiting the number of chromatographic dimensions to one (1D), the total

228   length of the chromatographic run, the amount of protein injected (as proteolytic digests), and a

229   single mass spectrometry injection rather than gas phase fraction approaches (Table S4). Each

230   laboratory group's specific approach is summarized in the supplemental methods, with

231   extraction in Table S5, and chromatography and mass spectrometry equipment and parameters

232   in Tables S6 and S7. While there are more sophisticated methods such as two-dimensional

233   (2D) chromatography and gas phase fractionations that have been demonstrated to provide

234   deeper metaproteomes (McIlvin and Saito, 2021), these often require specialized equipment

235   and/or additional instrument time. As a result, the study constraints were provided to ensure a

236   single simple method that all labs could utilize. Laboratories were invited to submit additional

237   data from more complex analytical setups if they first completed the 1D analyses.

238

239   *2.4 Compilation, analysis, and re-analysis of laboratory data submissions*

240   Results from individual laboratories' data submissions were analyzed in two ways as

241   shown in the flowchart of Figure 1a. First, submitted processed data reports (i.e. PSMs,

242   taxonomic, functional annotations) were compiled and interpreted. Second, raw data files (i.e.

243   spectra directly from instruments) from each group were put through a single bioinformatic

244   pipeline using SEQUEST HT/Percolator within Proteome Discoverer (Version 2.2.0.388,

245   Thermo Scientific) and Scaffold (Version 5.2.1, Proteome Software) to isolate variability

246   associated with bioinformatic processing. Note that Scaffold ignores the Percolator output from

247   Proteome Discoverer when re-running in Scaffold. This re-analysis (*single pipeline re-analysis*

248   hereon) allowed detailed cross-comparisons of laboratory practices to assess the influence of

249   the extraction and mass spectrometry components. Specific parameters of the latter included:

250   parent of tolerances of 10ppm were used on all instruments (all Orbitraps) for fragments

251   tolerances of 0.02 Da or 0.6 Da were used for Orbitrap ms2 instruments and for ion trap ms2

252   instruments, respectively. Fixed and variable modifications of +57 on C (fixed), and +16 on M

253   and +42 on Peptide N-Terminal (variable) were used. Peptide and protein FDRs (false

254   discovery rates) were set to lower than 1.0% using a decoy database, with 1 minimum peptide

255   per protein, and the resulting peptide FDR was 0.1%. The database used for PSMs was

256   Intercal_ORFs_prodigal_metagenemark.fasta based on the metagenomic sequencing

257   described above with 197,824 protein entries. The re-analysis was conducted within Scaffold

258   using total spectral counts and allowing single peptides to be attributed to proteins. In addition to

259   the total number of protein identifications, the number of protein groups identified by Scaffold

260   was also provided. Each protein group represented proteins identified with identical peptides,

261   collapsed into a single protein entry with the highest probability and number of spectral counts.

262

263   *2.5 Data analysis methods*

264   Several analyses were conducted using data from the single pipeline re-analysis. First,

265   pairwise comparisons of protein identifications were conducted using spectral abundance

266   reports produced in Scaffold, and loaded, analyzed and visualized in MATLAB (MathWorks Inc).

267   Two-way (independent) linear regressions were conducted using the script linfit.m. R^2 on the

268   seven datasets were averaged and their standard deviation calculated for shared proteins in

269   each dataset. Second, a Sørensen similarity (Sørensen, 1948) was calculated where a matrix

270   was generated that consisted of the unique proteins or peptides identified across all technical

271   replicates from the various labs with the relative abundance per replicate (% contribution of

272   each protein/peptide per technical replicate total). The Bray-Curtis dissimilarity pairwise distance

273   was calculated on this matrix using Python and the SciPy library (v. 1.4.1, (Virtanen et al.,

274   2020)) and then 1 – Bray-Curtis dissimilarity was calculated across the matrix to generate the

275   Sørensen pairwise similarity across all replicates. The resulting similarities per replicate were

276   clustered and visualized using the clustermap function in the Seaborn library (v. 0.10.0,

277   (Waskom, 2021)). Third, shared peptides and proteins were visualized using Upset plots, using

278   the R package UpSetR (Conway et al., 2017) to determine the number of unique peptide

279   sequences and annotated proteins in intersecting sets between all labs, all permutations of lab

280   subsets, and all lab pairs.

281   *2.6. Bioinformatics Intercomparison Methods*

282   The methods used for the bioinformatics intercomparison study are described by each

283   laboratory using their unique three-digit identifier code. All laboratories used the metagenomic

284   database generated in the laboratory study (see Section 2.2). **Lab 109:** The raw files were

285   searched against the metagenomic database employing a 2 round search using PEAKS Studio

286   X. The initial database search was performed to focus the metagenomic database for protein

287   sequences with peptide sequence matches at 5% FDR. The focused database was further used

288   for a second round search, which allowed a parent mass error tolerance of 10.0 ppm and a

289   fragment mass error tolerance of 0.6 Da. The search considered up to 3 missed cleavages,

290 carbamidomethylation as fixed and methionine oxidation and N-terminal acetylation as variable

291 modifications. The cRAP protein sequences (http://ftp.thegpm.org/fasta/cRAP./) were included

292 as contaminant database. Finally, PSMs were filtered for 1% FDR and annotated with

293 taxonomic lineages (obtained from the metagenomic experiments). Non-unique peptide

294 matches were annotated with the LCA of the respective lineages.

295 **Lab 321:** SearchGUI (Galaxy Version 3.3.10.1) was used to search using multiple search

296 algorithms (X!Tandem, MS-GF+ and Comet). For each search algorithm, Precursor Tolerance

297 of 10.0 ppm, Fragment Ion Tolerance of 0.6 Da and trypsin was used as an enzyme for

298 proteolytic cleavage. Searches were performed allowing for two missed cleavages fixed

299 modification of Carbamidomethylation at cysteine and Variable Modifications of Acetylation of

300 protein N-term and Oxidation of Methionine. PeptideShaker (Version: 1.16.36) was used to filter

301 peptides with the length of 8-50 aas and a precursor m/z tolerance of 10.0 ppm. Detected

302 peptide-spectral matches, peptides and proteins were reported at 1% global FDR. All of the

303 analysis was performed within Galaxy platform.

304 **Lab 321:** MaxQuant (Galaxy version 1.6.17.0+galaxy3) was used to search the datasets. A

305 fixed modification of carbamidomethylation at cysteine and variable mmodifications of

306 acetylation of protein N-term and oxidation of methionine was applied along with allowing for

307 two missed cleavages. The detection peptides and proteins were reported at 1% FDR.

308 **Lab 362:** The raw files were converted using ThermoRawFileParserGUI (version 1.4.1) to peak

309 lists (.mgf files) using "native Thermo library peak picking" as the peak picking option and

310 "Ignore missing instrument properties" as the error option. The peak lists (.mgf files) obtained

311 from MS/MS spectra were identified using X! Tandem version X! Tandem (Vengeance version

312 2015.12.1) using SearchGUI version 4.1.0. Here, the parameters provided and suggested by

313 the study were used: tolerances of 10 ppm for MS1 and 0.6 Dalton for MS/MS; dynamic

314 modifications: oxidation of M, and acetyl on N-terminus; static modifications: carbamidomethyl

315 of C. Identification was conducted against a concatenated target/decoy database of the

316 provided database.

317 The X!Tandem files were used as input in MS²ReScore

318 (https://github.com/compomics/ms2rescore), a machine learning-based post-processing tool

319 that improves upon Percolator rescoring of peptide-to-spectrum matches (PSMs). Here, the

320 search engine-dependent features of Percolator were appended with MS2 peak intensity

321 features by comparing the PSM with the corresponding MS²PIP-predicted spectrum. All

322 reported MS²ReScore PSM identifications have a q-value < 0.01. No protein grouping algorithm

323 was applied, and all identified taxa and functions are extracted from the provided database.

324 **Lab 458:** The Proteome Discoverer 2.5 platform was used (SequestHT + Percolator (MPS)).

325 Fully tryptic peptides with a minimum length of 6 peptides and a maximum of 2 missed

326 cleavages were required. Precursor Tolerance of 10.0 ppm, Fragment Ion Tolerance of 0.6 Da.

327 carbamidomethylation as fixed and methionine oxidation was set as a variable modification. Filtering

328 was performed at a 1% PSM- and peptide-level FDR. The MaxQuant contaminant list was used as

329 a contaminant database.

330 **Lab 501:** We first appended the database with a set of common contaminants (Global

331 Proteome Machine Organization common Repository of Adventitious Proteins). Then, we used

332 MSGF+ (Kim and Pevzner, 2014) to match mass spectra with peptide sequences, with cysteine

333 carbamidomethylation as a fixed modification, and methionine oxidation, glutamine modified to

334 pyro-glutamic acid, deamidated asparagine, and deamidated glutamine, as variable

335 modifications. Peptides were searched for with a Target-Decoy approach, with a 1% false

336 discovery rate at the peptide spectrum match level. For spectral counts, we summed MS2

337 spectra that identified a peptide, and normalized all spectral counts to the total spectral counts

338 per sample. Proteins were quantified using the median spectral count for all proteotypic

339 peptides (those peptides which uniquely correspond to a protein), specifically using the

340   OpenMS tool ProteinQuantifier. This approach requires at least one proteotypic peptide, but if

341   more are identified, those peptides are also used for quantification.

342   **Lab 828:** The raw files were analyzed using Thermal proteome discover. MS/MS spectrums

343   were searched against provided database using SEQUEST-HT engine. MS/MS spectra

344   searches were performed as follows: precursor ion tolerance of 10.0 ppm; fragment ion

345   tolerance of 0.6 Da; carbamidomethyl cysteine was specified as fixed modification, whereas

346   oxidation (M), deamidation (N/Q), and N-terminal protein acetylation were set as variable

347   modifications. Trypsin was specified as the proteolytic enzyme, allowing for two missed

348   cleavages. Percolator-based scoring was chosen to improve the discrimination between correct

349   and incorrect spectrum identifications, learning from the results of a decoy and target database;

350   settings were as follows: maximum delta Cn, 0.05; strict false-discovery rate of 0.01 and

351   validation based on q values.

352   **Lab 902:** SEQUEST-HT was used within Proteome Discoverer 2.2 using the following settings:

353   maximum missed cleavage 2, minimum peptide length 6, maximum peptide length 122,

354   precursor mass tolerance 10ppm, fragment mass tolerance 0.6 Dalton; dynamic modifications:

355   M oxidation, acetyl on N-terminus; static modifications: C carbamidomethyl. Percolator PSM

356   validator (within Proteome Discoverer) with following settings: maximum Delta Cn 0.05, target

357   FDR strict 0.01, target FDR relaxed 0.05, validation based on PEP. Scaffold 5.0 used to analyze

358   Proteome Discoverer generated files with following settings: scoring system: prefiltered mode;

359   protein grouping: standard experiment wide protein grouping; protein threshold 1.0% FDR;

360   peptide threshold 0.1% FDR; minimum number of peptides 1.

361   **Lab 932:** Mass spectrometry data were transformed from Thermo RAW format (version 66) to

362   mzML and Mascot Generic (MGF) formats using ThermoRawFileParser (version 1.2.0,

363   Hulstaert et al., 2020). Experimental metadata were extracted from mass spectrometry data

364   using the MARMoSET program (Kiweler et al. 2019). Mascot Server (version 2.6.2, Matrix

365   Science, LTD) software performed peptide-spectrum matching between experimental data and

366   a reference sequence database. Reference sequences included a total of 197,824 predicted

367   protein-coding ORFs from a metagenome assembly. Peptides matching an in-house curated

368   inventory of contaminant protein sequences, mass standards, and proteolytic enzyme

369   sequences were removed from the results. Mascot search parameters included the following

370   settings: +10.0 ppm monoisotopic precursor mass tolerance; +0.6 Da monoisotopic fragment

371   ion tolerance; one fixed modification (+57 to C residues); two variable modifications (+16 to M

372   residues, +42 to peptide amino-termini); digestion enzyme trypsin; two missed cleavages;

373   peptide charges +2-+7; and instrument type: electrospray ionization coupled to fourier-transform

374   ion cyclotron resonance (ESI-FTICR). Mascot search results containing peptide-spectrum

375   matches (PSMs) were exported for downstream data analysis. Scaffold Q+S (version 4.8.9) was

376   used to validate MS/MS-based peptide- and protein-level peptide-spectrum matches (PSM) with

377   the Peptide Prophet algorithm. Mascot PSM data were imported into Scaffold Q+S with the

378   following settings specified: quantitative metric: spectrum counting; scoring system: use legacy

379   Peptide Prophet scoring (high mass accuracy); protein grouping: use standard experiment-wide

380   grouping; optional loading steps: pre-compute false discovery rate (FDR) thresholds; and, use

381   local gene ontology (GO) annotations (UniProt GO annotation data retrieved 25 JUN 2020).

382   Scaffold Q+S identification criteria were set at greater/equals >99.9% probability by the Peptide

383   Prophet algorithm (Keller et al. Anal. Chem. 2002.) and >99.9% probability by the Protein

384   Prophet algorithm (Nesvizhskii et al., Anal. Chem. 2003) with >2 peptides at the protein level.

385   **Lab 957:** MSFragger 3.3 searches were performed with FragPipe 16.0 and Philosopher 4.0.0. A

386   concatenated target/reverse database was searched with a 50 PPM precursor and 0.4 Da

387   fragment mass tolerance. Automatic mass calibration and parameter optimization was enabled

388   and precursor mass errors for up to +2 neutrons were considered. Peptide candidates were

389   generated from database protein sequences assuming tryptic digestion, allowing for up to one

390   missed cleavage. Peptides were required to have between 8-50 amino acids and range from

391   500 to 5000 m/z. Cysteines were assumed to be fully carbamidomethylated, and peptides were

392 searched considering variable n-terminal pyroglutamic acid formation and methionine oxidation.

393 PeptideProphet was used for FDR validation with the following default options: "--decoy probs",

394 "--ppm", "--accmass", "--nonparam", and "--expectscore", which allow for additional high-mass

395 accuracy analysis and non-parametric distribution fitting. ProteinProphet was used for protein-

396 level FDR validation with the following default option: "--maxppmdiff 2000000". Filtering was

397 performed using a 1% peptide-level and a 1% protein-level FDR threshold.

398 **3. Results**

399 *3.1 Experimental Design*

400   This ocean metaproteomic intercomparison consisted of two major components: a

401 laboratory component, where independent labs processed identical ocean samples

402 simultaneously collected from the North Atlantic Ocean (Fig. 1a, see Section 2.1), and a

403 subsequent bioinformatic component. Participating institutions and persons at those institutions

404 are listed in Table S1, with all participants also listed as co-authors. Both arms of the study were

405 conducted under blinded conditions, where correspondence with participants was conducted by

406 an individual not involved in either study, and submitted results and data were anonymized prior

407 to sharing with the consortium. Within both arms of the study, participants were provided the

408 location of the study site and metadata about the sampling locations, time and depth at the

409 onset of the study. The laboratory study involved two biomass-laden filter slices collected from

410 the North Atlantic Ocean Bermuda Atlantic Time series Study site at 80m depth being sent to

411 each participating group for protein extraction, mass spectrometry, and bioinformatic analyses

412 (see Section 2.1). This depth was chosen to correspond to a depth with abundant chlorophyll

413 and associated photosynthetic organisms. The bioinformatic effort was independent of the

414 laboratory effort and involved the distribution and bioinformatic analysis of two metaproteomic

415 raw data files generated from samples also from the North Atlantic Ocean upper water column

416 BATS station (20m and 120m depths, see Section 2.1). These depth were chosen to reflect the

417   near surface (high-light) and deep chlorophyll maximum (low-light) communities present in the

418   stratified summer conditions.These files were distributed after labs had submitted their

419   laboratory extracted raw data files. The raw files from the bioinformatic study were distinct from

420   the samples used in the laboratory intercomparison study to avoid any biases from groups that

421   analyzed those samples previously. Submitted results from both components were anonymized

422   and assigned three-digit lab identifiers generated randomly with laboratory and bioinformatic

423   results from the same lab being assigned distinct identifiers.

424   We report results for two study components: Part 1 (Section 3.2) involves the data

425   generation intercomparison of distributed subsamples from the North Atlantic Ocean (Fig. 1;

426   Section 2.1). Part 2 (Section 3.3) was an bioinformatic intercomparison, where metaproteomic

427   raw files were shared with participants and processed results were submitted. Both components

428   were conducted as blinded studies, where each dataset was assigned a three digit randomly

429   generated identifier, with those identifiers used throughout the Results and Discussion.

430

431   *3.2 Mass Spectrometry Data Generation Intercomparison*

432   Nine laboratories submitted raw and processed datasets from the analysis of the

433   distributed Atlantic Ocean field samples (Table S1). The processed data submissions were

434   heterogeneous in output formats, statistical approaches, and parameter definitions. Because of

435   the challenges of comparing data derived from different types of statistical approaches used for

436   peptide and protein identification and inference, as well as the varying output formats from

437   various software packages, the user-generated data submissions were difficult to compile and

438   compare, resulting in variability in the number of identifications depending on the statistical

439   approaches and thresholds applied. These results are further discussed in the Supplemental

440   Section (Figure S1, Table S8). Despite these challenges, an average of 7142 +/- 2074 peptides

441   were identified across the pairwise comparisons (Figure S1c) representing 20% of the 35,715

442 total unique peptides detected across all labs. Together these findings implied a consistency of

443 peptide identifications across participants. The variability in proteome depth reflected the

444 combination of differing parameters employed by software and laboratory approaches.

445   To remove this variability associated with user-selected bioinformatic pipelines, a single

446 pipeline re-analysis of the submitted raw mass spectral data was conducted. Raw data files

447 were processed together within a single bioinformatic pipeline consisting of SEQUEST-HT,

448 Percolator, and Scaffold software and evaluated to a false discovery rate threshold of < 0.1% for

449 peptides and 1.0% for proteins (see Section 2.4). Two datasets were found to have had issues

450 during extraction and analysis that affected the results in both processed and raw data (Labs

451 593 and 811; Table S8). Notably these two laboratories differed from the others in that they did

452 not use SDS as a protein solubilizing detergent (Table S5). This likely resulted in inefficient

453 extraction of the bacteria that dominated the sample biomass (e.g. picocyanobacteria and

454 *Pelagibacter*) embedded within the membrane filter slices. Further examination showed

455 polyethylene glycol contamination of one dataset (Lab 811) and low yield from sample

456 processing and extraction from the other (Lab 593). As a result, those datasets were not

457 included in the single pipeline re-analysis. The standardized pipeline included calculations of

458 shared peptides and proteins, quantitative comparisons, and consistency of taxonomic and

459 functional results.

460   The total number of peptide and protein identifications and PSMs in the single

461 bioinformatic pipeline analysis varied by laboratory (Table S9), with unique peptides ranging by

462 more than a factor of 3 from 3,354 to 16,500, and with 27,346 total unique peptides identified

463 across laboratories. This variability was likely due to different extraction, chromatographic, and

464 mass spectrometry hardware and parameters employed used by each laboratory, resulting in a

465 varying depth of metaproteomic results. Yet, as with the user-submitted results, there was

466 considerable overlap in identifications between all datasets. An intersection analysis found the

467 numerous shared peptides between all combinations of laboratories, with 1,395 peptides shared

468   between all seven laboratory datasets (Figure 2a). Laboratories with deeper proteomes shared

469   numerous peptides, for example the two laboratories with the most discovered unique peptides

470   shared ~3000 peptides between them, implying that shared peptides is a useful metric for

471   intercomparability. They also had the largest numbers of peptides that were not found by any

472   other labs (3617 and 2819, respectively). The fourth largest intersection size (1395) represented

473   the unique peptides discovered by all labs. Beyond that there were 12 different groupings of

474   peptides that were shared among at least four laboratories. Consistent with this, 3-way Venn

475   diagrams of labs 135, 209 and 438 had an intersection of 2398 peptides, labs 652, 729, and 774

476   shared 3016 peptides, and labs 127, 135, and 309 shared 2304 peptides (Figure 2d).

477   A similar analysis was conducted at the protein level, where the number of proteins

478   identified (see Section 2. Methods) identified 8,043 unique proteins in total across all

479   laboratories, with 1,056 proteins of those observed in all seven labs (see 7-way Venn diagram in

480   Figure 2c). Three-way Venn diagram comparisons among labs 135, 209 and 438 had an

481   intersection of 1,254 proteins, and labs 652, 729, and 774 shared 1,925 proteins (data not

482   shown).

483   Optional deeper metaproteome results were submitted by three laboratories using either

484   a long gradient of 12 hours or 2 dimensional chromatographic methods (Table S10). The

485   number of discovered peptide and protein identifications were higher in each case, with as

486   many as 18477 unique peptides and 7765 protein identifications from an online 2-dimensional

487   chromatographic analysis from a 5 μg single injection.

488   The mapping of identified peptides to protein sequences forms the basis for protein

489   identifications in the form of DDA bottom-up proteomics employed here. The relationship

490   between peptides and protein identification was explored in Figure 3 and found to be correlated

491   by two-way linear regression with R^2 values of 0.97 and 0.98 for total protein identifications and

492   protein groups, respectively. Together, the fact that there is a linear relationship between

493   peptides and proteins across all laboratories (including labs employing deeper methods) could

494 imply that the number of protein identifications has not begun to plateau and reached

495 'saturation', likely due to the immense biological diversity and abundance of lower abundance

496 peptides within these samples. This approach has some similarities to rarefaction curves used

497 in metagenomic sequencing to determine if the majority of species diversity has been sampled,

498 although in this case number of peptides used as a metric for sampling depth instead of

499 additional number of DNA sequencing samples typically used for rarefaction curves. This

500 indicated that with deeper depth of analysis by some laboratories, there was no fall off in the

501 increase in protein identifications that might be attributed to additional peptides mapping to

502 already discovered protein sequences. In addition, the 2D and long gradient additional analyses

503 conducted by several laboratories fell upon this line consistent with this "more peptides – more

504 proteins" observation, implying more room for improvements in depth of metaproteomic

505 analyses.

506   A quantitative analysis of spectral counts from the wet lab re-analysis showed broad

507 coherence among the seven laboratories. Pairwise comparisons of protein spectral counts were

508 conducted for each of the seven labs against the other six (visualized in a 7x7 matrix, with

509 duplicate comparisons removed (e.g., A vs B and B vs A)), where each data point reflects the

510 spectral counts for a protein shared between laboratories (Figure 4a). When a dataset was

511 compared with itself a unity line of datapoints was observed along the diagonal axis as

512 expected. Two-way linear regressions were conducted on each of these pairwise comparisons.

513 The slopes ranged from 0.33 to 5.5 (Figure S2), implying a varying dynamic range in spectral

514 counts across laboratories, likely due to variations in instrument parameterizations selected by

515 each laboratory, and consistent with the lack of normalization between laboratories. The

516 coefficient of determination R^2 values from 0.43 to 0.84 with an average of 0.63 +/- 0.11,

517 showing coherence among results for these large metaproteomic datasets (Figure 4b, Table

518 S12). To provide a sense of coherence of each laboratory to the others, the R^2 values of a lab

519 against the other six laboratories were averaged and the standard deviation calculated. All of

520   these average R^2 values were higher than 0.5, which showed overall quantitative consistency

521   despite the size and complexity of these datasets (Figure 4d).

522   A comparative taxonomic and functional analysis was also conducted using a single

523   bioinformatic pipeline (see metagenomic sequencing methods for annotation pipeline). Lowest

524   common ancestor (LCA) analysis of peptides identified from datasets from seven laboratories

525   showed consistent patterns of taxonomic distribution using the MetaTryp package (Figure 5a;

526   (Saunders et al., 2020). Cyanobacteria and alphaproteobacteria were the top two taxonomic

527   groups in all laboratory submissions, consistent with the abundant picocyanobacteria

528   *Prochlocococcus* and the heterotrophic bacterium *Pelagibacter ubique* known to be dominant

529   components of the Sargasso Sea ecosystem (Sowell et al., 2009; Malmstrom et al., 2010). For

530   example, *Prochlorococcus* is consistently present between 10^4 and 10^5 cells per milliliter in this

531   region and has been observed to contribute to carbon export from the euphotic zone (Casey et

532   al., 2007). *Pelagibacter* cells can also be in excess of 10^5 cells per milliliter at the BATS North

533   Atlantic location (Carlson et al., 2009). These results are broadly similar to the representation of

534   phyla within the metagenome annotations, where Proteobacteria (including *Pelagibacter*) and

535   Cyanobacteria (including *Prochlorococcus* and *Synechococcus*) were major components,

536   although Bacteriodetes (including Flavobacteria) are more prevalent in the metagenome

537   annotations than in the metaproteome. Some differences may also be due to the incorporation

538   of protein abundances in Fig 5a, versus simple taxonomic attribution of non-redundant

539   assembled open reading frames in the metagenome analysis, as well as the use of multiple

540   sequencing platforms and gene calling algorithms (Section 2.2, Figure S4).

541   Similarly, KEGG Orthology group (KO) analysis of those datasets also showed highly

542   similar patterns of protein functional distributions across laboratories (Figure 5b). Notably the

543   PstS phosphate transporter protein from *Prochlorococcus* was the most abundant protein in all

544   datasets, consistent with observations of phosphorus stress in the North Atlantic oligotrophic

545   gyre and its biosynthesis in marine cyanobacteria (Scanlan et al., 1997; Coleman and Chisholm,

546   2010; Ustick et al., 2021). These findings demonstrate the reproducibility in the primary

547   functional and taxonomic conclusions from the metaproteome datasets. Finally, a Sørensen

548   similarity analysis of the 1,000 proteins with highest spectral counts revealed 70–80%

549   similarities between most laboratory groups in the data re-analysis (Figure 6). When conducted

550   on the full dataset with all peptides and proteins, the Sørensen similarity analyses showed

551   peptides had lower similarity than proteins, implying variability is ameliorated when aggregated

552   to the protein level (Figure S3).

553

554   *3.3. Bioinformatic Data Analysis Intercomparison*

555   Two metaproteomic raw files were provided to intercomparison participants and were

556   searched with each laboratory's preferred database searching bioinformatic pipeline. The

557   samples that generated the data for these files were collected by autonomous AUV *Clio* during

558   a single dive at the Bermuda Atlantic Time-series Study Station (Breier et al., 2020), and were

559   distinct from the samples associated with the laboratory intercomparison component. However,

560   they were also from the North Atlantic Ocean, allowing the same metagenomic database to be

561   used. This database was not collected simultaneously with the bioinformatics samples, so it was

562   not as representative as that used in the laboratory intercomparison. However, the BATS study

563   region is known to maintain similar major taxonomic composition throughout the year (e.g.,

564   *Prochlorococcus* and SAR11, see discussion in Section 3.2), hence enabling many protein

565   identifications. This bioinformatic study component was not launched until after the laboratory-

566   based intercomparison submission deadline to avoid influencing that part of the study by

567   sharing similar raw data. Samples were named Ocean 8 and Ocean 11 and were taken from

568   120 m and 20 m depths, respectively.

569   The bioinformatic intercomparison involved 10 laboratories utilizing 8 different software

570   pipelines including the PSM search engines: SEQUEST, X!Tandem, MaxQuant, MSGF+,

571   Mascot, MSFragger, and PEAKS (Table S11, see Methods Section 2.6). As with the user

572   supplied laboratory results, the results were challenging to compile due to different types of data

573   outputs, approaches used in protein inference, and statistical approaches applied within each

574   pipeline. Unique peptide discoveries served as a useful base unit of comparison that were less

575   subject to these comparison challenges. The number of peptides ranged from 1724 to 6369 in

576   Ocean 8 and 3019 to 8288 in Ocean 11 (Figure 7; Table S11). The differences in the number of

577   peptides was likely due to parameters used in software, for example, laboratory 932 had the

578   lowest number of peptides identified in both samples, but also used a highly stringent 99.9%

579   probability cutoff that likely influenced this result.

580

581   **4. Discussion**

582   *4.1 Assessment of Ocean Metaproteomics Reproducibility*

583   Given the recent establishment of complex metaproteomic techniques, intercomparisons

584   are valuable in demonstrating their suitability for ocean ecological and biogeochemistry studies.

585   Synthesizing the results of the laboratory and mass spectrometry blinded intercomparison study

586   (Section 3.2) processed with a single bioinformatic pipeline (Section 2.4), we observed

587   consistent reproducibility with regards to three attributes of ocean metaproteomics analyses: 1)

588   the identity of discovered peptides and proteins (Fig. 2), 2) their relative quantitative

589   abundances (Figs. 4 and 6), and 3) the taxonomic and functional assignments within

590   intercompared samples (Fig 5). With over 1000 proteins identified across seven laboratories

591   and Sørensen similarity indexes typically higher than 70–80% (Fig. 6), the results demonstrate

592   consistent detection and quantitation of major proteins in the sample. These results provide

593   confidence that multiple laboratories can generate reproducible results describing the major

594   proteome composition of ocean microbiome samples to assess their functional and

595   biogeochemical activity .

596   While there is good agreement, this congregation of data allows further exploration of

597   the influence of methods on the results. In particular, as mentioned above the range of pairwise

598   comparisons had correlation coefficients ranging from 0.43 to 0.84, with most values falling

599   between 0.6 and 0.8 (Figure 4b and 4e; Table S12). This average of all correlation coefficients

600   described above (0.63 +/- 0.11) implied good reproducibility between laboratories in general.

601   We can explore what might have influenced the variability and lower range of coefficients. The

602   correlation coefficients of lab 209 had two of the three R^2 values below 0.499 in pairwise

603   comparisons (0.431 and 0.475), yet also had values that ranged from 0.61 to 0.70. Why would

604   this variability exist? Lab 209 's methods differed from other labs in several ways: they used the

605   oldest and slowest instrument of the group (Thermo Orbitrap Elite), used CID instead of HCD for

606   fragmentation and rapid scan mode, and used an unusually long column of 200cm to

607   compensate for the older instrument (Table S6). As a result, lab 209 had the lowest number of

608   peptide (3354) and protein (1586) ID's of the seven labs (Table S9), which was several fold

609   lower than the lab with the highest number and reduced the number of shared peptides across

610   all laboratories. In pairwise comparisons, lab 209 had the lowest number of shared peptides at

611   an average of 1304. Interestingly however, lab 209 did not have the lowest number of total

612   spectral counts (63198), being close to the average (70843 +/- 27455), implying that more

613   abundant peptides were detected relative to rarer ones.

614   We initially suspected the lower R^2 values in pairwise comparisons with lab 209 may

615   have been related to comparisons to laboratories with similarly lesser peptide depth, but this

616   was not the case: the two lowest correlation coefficients for lab 209 were with laboratories 135

617   and 774 (the 0.431 and 0.475 values), the latter of which had the highest number of peptide

618   identifications. The answer for this difference in quantitative values maybe within the selection of

619   parameters used to sample peptide peaks: Both lab 135 and 774 used 60 second dynamic

620   exclusion, whereas the other 5 labs used dynamic exclusions between 10 and 30 seconds in

621 length (Table S7). This higher dynamic exclusion likely contributed to providing greater peptide

622 discovery depth, but at the cost of quantitative consistency with other laboratories, since this

623 parameter selects against repeat counting of abundant peaks and would reduce spectral counts

624 of the more abundant peptides that lab 209 was detecting. This result demonstrates the

625 influence of the mass spectrometer parameters in quantitative reproducibility when using global

626 proteomic DDA mode.

627 *4.2 Metrics in metaproteomics: Core versus rare "long tail" proteins*

628   While abundant proteins were consistently detected across seven laboratories'

629 submissions, there was substantial variability in the less abundant proteins (Fig. 2). This is

630 evident in Figure 8, where most of the 1063 proteins across seven laboratories in the re-

631 analysis were in the upper half of proteins when ranked by abundance. This simultaneous

632 consistency in abundant proteins and diversity in rare proteins (and their respective peptide

633 constituents) was likely a result of several factors. First, the intercomparison experimental

634 design stipulated 1D chromatography in order to provide straightforward comparisons that all

635 laboratories could accomplish. This contributed to study consistency, but also resulted in lesser

636 proteome depth compared to more elaborate methods such as 2D chromatography and gas

637 phase fractionation commonly in use. Second, the sample complexity of ocean metaproteomes

638 has been shown to be enormous, with a far greater number of low abundance peptides present

639 than HeLa human cell lines (Saito et al., 2019). The combined effect of these factors meant that,

640 while laboratories were able to detect abundant proteins consistently, there was considerable

641 stochasticity associated with the detection of less abundant peptides resulting in a long tail of

642 discovered lower abundance proteins.

643   Mass spectrometer settings such as dynamic exclusion, chromatography conditions, and

644 variation in sample preparation methods all likely contributed to this stochastic variability in rare

645 peptide detection among laboratories. Moreover, while all participating laboratories used

646 Thermo orbitrap mass spectrometers, there were seven variants of instrument model, including

647 some with Tribrid multiple detector capability (Table S6). While testing other mass spectrometry

648 platforms is of interest, this trend of community orbitrap usage in this study is consistent with the

649 broader proteomics community, where currently 9 of the top 10 instruments used in

650 ProteomeXchange consortium repository data submissions utilize orbitraps as of the manuscript

651 submission date (Deutsch et al., 2019). When conducting analysis of environmental samples,

652 choices can be made about instrument setup and parameters based on the scientific objectives,

653 for example if maximal proteome depth or robust quantitation while using a discovery approach

654 is desired. Future intercalibration efforts enlisting more sensitive metaproteomic methods such

655 as 2D-chromatography (McIlvin and Saito, 2021), more sensitive instruments (Stewart et al.,

656 2023), and other emerging methods can greatly improve detection and quantitation of rarer

657 proteins in metaproteomes, allowing exploration of the depths of state-of-the-art capabilities

658 rather than our present emphasis on interlaboratory consistency. Moreover, the development

659 and adoption of best practices in sample collection, extraction, chromatographic separation,

660 mass spectrometry analyses, and bioinformatic approaches will contribute to interlaboratory

661 consistency.

662 *4.3* Despite the inter-laboratory variability in the detected sets of rarer peptides and proteins, we

663   interpret these to be largely robust identifications. The stringent 0.1% peptide-level FDR

664   threshold we use here is determined by scoring decoys: reverse sequenced peptides that

665   are not in our samples. Peptide assignments to these decoys model the score distribution of

666   all incorrect peptide-spectrum matches (PSMs) in our study such that FDRs can be

667   estimated in an unbiased way for each laboratory. However, these estimates are

668   complicated by subtle sequence diversity within a population's proteome, which is typically

669   not considered by proteomics software designed to analyze single species (Schiebenhoefer

670   et al., 2019). This diversity within metaproteomic samples results in the presence of highly

671   similar peptides with nearly identical precursor masses that produce many of the same b-

672   and y-ions, and this similarity is not well modeled by decoy peptides. The influence of

673   microdiversity on metaproteomics FDR estimation using strain-specific proteogenomic

674   databases is an important area of future exploration (Wilmes et al., 2008).*Bioinformatics*

675   *Intercomparison Assessment*

676   The discovery of peptide constituents of proteins within a complex ocean metaproteomic

677   matrix was successful across all software packages tested (Figure 7), where the metric for

678   success is a comparable number of peptide identifications. This is a notable finding due to the

679   highly complex mass spectra, large number of chimeric peaks present (Saito et al., 2019), and

680   large database sizes involved in ocean metaproteomes. To our knowledge, some of these

681   software packages had not yet been applied to ocean metaproteomes. There was also

682   variability associated with the stringency of statistical parameters employed, which points to the

683   challenges in assembling datasets from multiple laboratories with different depth of proteome

684   identifications.

685   Despite the success of this intercomparison component across software packages, there

686   is likely considerable room for improvement in the future. As mentioned previously, ocean

687   samples are highly complex and there are likely additional peptides that remain unidentified

688   using current technology, due to low intensity peaks and co-elution with other peptides resulting

689   in the chimeric spectra. Significant improvements in depth of analysis can be achieved through

690   increased chromatographic sample separation and optimized (or alternative) mass spectrometry

691   data acquisition strategies. Yet there is room for bioinformatic improvements as well: most DDA

692   database searching algorithms are unable to identify multiple peptides within a single

693   fragmentation spectrum. Moreover, when in DDA collection mode mass spectrometry software

694   typically does not isolate and fragment peptides that cannot be assigned a charge state, which

695 is a common occurrence for the low abundance peaks within ocean samples. As a result, there

696 is considerable room for improvements in bioinformatic pipelines to discover additional peptides.

697 Although the application of data independent approaches (DIA) to oceanographic

698 metaproteomics analysis has been limited (e.g. Morris et al., 2010), the systematic nature of ion

699 selection and fragmentation allows for a greater number of low abundant peptides to be

700 quantified when enough ions can be isolated to produce robust MS2 spectra.,.

701 *4.4 Lessons Learned and Future Efforts in Ocean Metaproteomic Intercomparisons and*

702 *Intercalibrations*

703 As the first interlaboratory ocean metaproteomics study, we chose to describe this study

704 as an intercomparison rather than an intercalibration and it served as a vehicle with which to

705 assess the extent of reproducibility. There were several lessons learned that can be

706 summarized here. These include the efficacy of a SDS detergent and heat treatment in lysing

707 and solubilizing marine microbial cells embedded on membrane filters, the significant problem

708 of data intercomparability between PSM software outputs and need for data output

709 standardization, and the influence of different hardware capabilities (Orbitrap generation) and

710 their parameter settings such as dynamic exclusion on proteome depth and quantitative

711 comparisons of spectral counts. The development of best practices associated with sample

712 collection, extraction, and analysis would be valuable, while also encouraging methodological

713 improvements and backward compatibility through the use of reference samples.

714 Future intercalibration efforts could aim to further assess and improve upon the level of

715 accuracy, reproducibility, and standardization of ocean metaproteome measurements. In

716 particular, alternative modes of data collection and quantitation could also be tested in future

717 interlaboratory comparisons, including parallel reaction monitoring mode (PRM), multiple

718 reaction monitoring mode (MRM), quantification using isotopic labeling or tagging, and DIA

719   methods. PRM and MRM methods allow sensitive targeted measurements of absolute

720   quantities of peptides (e.g. copies per liter of seawater in the ocean context). As many 'omics

721   methodologies applied in environmental settings operate in relative abundance modes, adding

722   the ability to measure absolute quantities would be particularly valuable for comparisons of

723   environments across space and time. Targeted metaproteomic methods have been deployed in

724   marine studies using stable isotope labeled peptides for calibration, achieving femtomoles per

725   liter of seawater estimates of transporters, regulatory proteins, and enzymes (Saito et al., 2020;

726   Bertrand et al., 2013; Saito et al., 2014, 2015; Joy-Warren et al., 2022; Wu et al., 2019). These

727   methods are not yet widely adopted, but with growing interest could be deployed to other

728   laboratories and incorporated into future iterations of intercomparison and intercalibration

729   studies. DIA also has great potential in ocean metaproteome studies and is increasingly being

730   deployed in laboratory and field studies of marine systems. Similar to this DDA intercomparison,

731   the methodological and bioinformatic challenges of DIA could be explored during

732   intercomparisons of analyses of ocean samples. Finally, as mentioned above, all participants of

733   this study used orbitrap mass spectrometers for DDA submissions, but new instrumentation

734   such as trapped ion mobility spectrometry time of flight mass spectrometers (timsTOF) may be

735   applied to ocean metaproteome analyses and would be important to intercompare with orbitrap

736   platforms.

737   As noted above, there were also challenges in collating and comparing data outputs

738   from various software, as well as variation in how those programs conducted protein inference.

739   For example, peptide-level data from different research groups were reported as either

740   unmodified peptide sequences or as various peptide analytes (where modifications and charges

741   states were included with the peptide sequence), making compilation of peptide reports difficult.

742   Similarly, at the protein level reported proteins could be counted either before or after protein

743   grouping, e.g. applying Occam's-razor logic to peptide groupings into proteins – the former

744 reflecting the set of all proteins in the database that could be in the sample, the latter the

745 minimum set required to explain the peptide data. Such issues will also contribute to challenges

746 in integration and assembly of data from different laboratories for large ocean datasets. While

747 best practices for metadata and data types have been described by the community that include

748 specific attributes important for environmental and ocean samples such as geospatial location

749 and sample collection information (Saito et al., 2019) similar to the metadata standard recently

750 put forward in the human proteome field (Dai et al., 2021), this study also demonstrated that

751 there is a need for standardization of data output formats for metaproteomic results.,.

752 *4.5 Metaproteomics in Global Ocean Surveys*

753 Understanding how the oceans are responding to the rapid changes driven by human

754 alteration of ecosystems is a high priority. Ocean and environmental sciences have a long

755 history of chemical measurements that are critical to assessing ecosystems and climatic

756 change. Such measurements have been straightforward for discrete measurements, such as

757 temperature, pH, chlorophyll, phosphate, dissolved iron and numerous other variables. When

758 collected over large spatial (ocean basin) or temporal (seasonal or decadal spans) scales, these

759 datasets have been powerful in identifying major (both cyclical and secular) changes. 'Omics'

760 measurements represent a more complex data type where each discrete sample can generate

761 thousands (if not more) of units of information. This study demonstrates the power and potential

762 for collaborative metaproteomics studies to identify key functional molecules and relate them to

763 their taxonomic microbial sources within the microbiome from multiple lab groups. Moreover,

764 multi-lab metaproteomics results in vastly enhanced identification of low abundance proteins

765 that are not identified by all research groups. Such low abundance proteins can be more likely

766 to change in abundance with changing environmental conditions and nutrient limitations,

767 resulting in a more nuanced and richer investigation of marine microbial ecology and

768 biogeochemistry with collaborative metaproteomics research. The implementation of such

769   voluminous data is beginning to be applied on larger scales and holds great promise in

770   improving not only our understanding of the functioning of the current system, but also the way

771   we assess how environments are changing with continued human perturbations.

772   Intercomparison and intercalibration are critical activities to undertake in order to allow

773   comparison of 'omics results across time and space dimensions. With major programs

774   underway and being envisioned such as the BioGEOTRACES, AtlantECO, Bio-GO-SHIP, and

775   BioGeoSCAPES efforts, the imperative for such intercalibration has grown and the need for best

776   practices is urgent. This Ocean Metaproteomic Intercomparison study is a valuable step in

777   assessing metaproteomic capabilities across a number of international laboratories,

778   demonstrating a clear consistency in measurement capability, while also pointing to the

779   potential for continued community development of metaproteomic capacity and technology.

780

781   *Author Contributions***:** MAS and MRM obtained OCB workshop support and drafted the

782   experimental design with feedback from BN, MJ, and DL acting as the Advisory Committee. SC,

783   JH, DL, GJV, and JKS conducted the metagenomic analyses and assembly. JKS, MAS, MMB,

784   MRM, and RM conducted data analysis and visualization. MRM, MAS, JAB, MVJ, and RJ

785   conducted sample collection and/or AUV Clio operations. MAS, JKS, MRM, EMB, SC, JRC, TG,

786   JH, RLH, PJ, MJ, RK, HK, DL, JSPM, EM, SM, DMM, JN, BN, JJ, MD, GJH, RG, RM, BLN, MP,

787   SP, AR, ER, BS, TVDB, JRW, HZ, and ZZ contributed mass spectrometry data and/or

788   bioinformatics data for the intercomparison. JKS anonymized data submissions and conducted

789   follow-up correspondence about methods. The manuscript was drafted by MAS and all authors

790   contributed to the writing and editing.

791

792   *Data and Code Availability:* The raw files, metagenome database

793   (Intercal_ORFs_prodigal_metagenemark.fasta), and associated annotations

794   (Intercal_assembly_annotations.csv) for this project summarized in Table S3 are available at

795   ProteomeXchange and PRIDE repository with the dataset identifier PXD043218

796   (https://www.ebi.ac.uk/pride/archive/projects/PXD043218) and PXD044234

797   (https://www.ebi.ac.uk/pride/archive/projects/PXD044234). Co-located information about these

798   datasets are available at the Biological and Chemical Data Management Office under project

799   765945 (https://www.bco-dmo.org/project/765945) and at the BATS page (https://www.bco-

800   dmo.org/project/2124). The metagenomic reads are listed under Bioproject Accession:

801   PRJNA932835; SRA submission: SUB12819843, available at link:

802   https://www.ncbi.nlm.nih.gov/bioproject/PRJNA932835. The code for upset visualization is

803   available at: https://maggimars.github.io/protein/PeptideUpSetR.html.

804

805   *Competing Interests* - The authors declare no competing financial interests.

806   *Supplemental Materials* - Methods for the bioinformatic intercomparison study are available in

807   the Supplemental Methods. Supplemental Informational is available as Tables S1-S11, and

808   Figures S1-S3.

809   *Acknowledgements* - This manuscript is a product of the sustained efforts of a small group

810   activity supported by the Ocean Carbon & Biogeochemistry (OCB) Project Office (NSF OCE-

811   1850983 and NASA NNX17AB17G), based on a proposal written by M.A.S. and M.R.M. The

812   research expedition where samples were collected was supported by the NSF Biological

813   Oceanography and Chemical Oceanography. We also thank the R/V *Atlantic Explorer* and the

814   Bermuda Atlantic Time-series Study team for assistance at sea. AUV Clio sample collection was

815   supported by NSF OCE 1658030 and 1924554. Analyses by participating laboratories

816   acknowledge support from: NSERC Discovery Grant RGPIN-2015-05009 and Simons

817   Foundation Grant 504183 to E.M.B, the Austrian Science Fund (FWF) DEPOCA (project

818   number AP3558721) to G.J.H., Simons Foundation grant 402971 to J.R.W., National Institute of

819   Health 1R21ES034337-01 to B.L.N., the Norwegian Centennial Chair Program at the University

820   of Minnesota for funding to PDJ, SM, and TJG, NIH R01 GM135709, NSF OCE-1924554, OCE-

821   2019589 and Simons Foundation Grant 1038971 to M.A.S. Identification of certain commercial

822   equipment, instruments, software, or materials does not imply recommendation or endorsement

823   by the National Institute of Standards and Technology, nor does it imply that the products

824   identified are necessarily the best available for the purpose. We thank Magnus Palmblad, John

825   Kucklick, and an anonymous reviewer for comments on the pre-submission version of the

826   manuscript. We also thank two anonymous reviewers for their constructive comments during

827   manuscript review.

828

829

830

References

831 Bender, S. J., Moran, D. M., McIlvin, M. R., Zheng, H., McCrow, J. P., Badger, J., DiTullio, G.
833 R., Allen, A. E., and Saito, M. A.: Colony formation in Phaeocystis antarctica: connecting
834 molecular mechanisms with iron biogeochemistry, Biogeosciences, 15, 4923–4942, 2018.

835 Bergauer, K., Fernandez-Guerra, A., Garcia, J. A., Sprenger, R. R., Stepanauskas, R.,
836 Pachiadaki, M. G., Jensen, O. N., and Herndl, G. J.: Organic matter processing by microbial
837 communities throughout the Atlantic water column as revealed by metaproteomics, Proceedings
838 of the National Academy of Sciences, 115, E400–E408, 2018.

839 Bertrand, E. M., Moran, D. M., McIlvin, M. R., Hoffman, J. M., Allen, A. E., and Saito, M. A.:
840 Methionine synthase interreplacement in diatom cultures and communities: Implications for the
841 persistence of B12 use by eukaryotic phytoplankton, Limnology and Oceanography, 58, 1431–
842 1450, 2013.

843 Breier, J. A., Jakuba, M. V., Saito, M. A., Dick, G. J., Grim, S. L., Chan, E. W., McIlvin, M. R.,
844 Moran, D. M., Alanis, B. A., and Allen, A. E.: Revealing ocean-scale biochemical structure with a
845 deep-diving vertical profiling autonomous vehicle, Science Robotics, 5, eabc7104, 2020.

846 Buchfink, B., Xie, C., and Huson, D. H.: Fast and sensitive protein alignment using DIAMOND,
847 Nature methods, 12, 59–60, 2015.

848 Carlson, C.A., Morris, R., Parsons, R., Treusch, A.H., Giovannoni, S.J. and Vergin, K., 2009.
849 Seasonal dynamics of SAR11 populations in the euphotic and mesopelagic zones of the
850 northwestern Sargasso Sea. The ISME journal, 3(3), pp.283-295.

851 Casey, J.R., Lomas, M.W., Mandecki, J. and Walker, D.E., 2007. Prochlorococcus contributes
852 to new production in the Sargasso Sea deep chlorophyll maximum. Geophysical Research
853 Letters, 34(10).

854 Cohen, N. R., McIlvin, M. R., Moran, D. M., Held, N. A., Saunders, J. K., Hawco, N. J.,
855 Brosnahan, M., DiTullio, G. R., Lamborg, C., and McCrow, J. P.: Dinoflagellates alter their
856 carbon and nutrient metabolic strategies across environmental gradients in the central Pacific
857 Ocean, Nature Microbiology, 6, 173–186, 2021.

858 Cohen, N. R., Krinos, A. I., Kell, R. M., Chmiel, R. J., Moran, D. M., McIlvin, M. R., Lopez, P. Z.,
859 Barth, A., Stone, J., Alanis, B. A., Chan, E. W., Breier, J. A., Jakuba, M. V., Johnson, R.,
860 Alexander, H., and Saito, M. A.: Microeukaryote metabolism across the western North Atlantic
861 Ocean revealed through autonomous underwater profiling, Ecology,
862 https://doi.org/10.1101/2023.11.20.567900, 2023.

863 Coleman, M. L. and Chisholm, S. W.: Ecosystem-specific selection pressures revealed through
864 comparative population genomics, Proceedings of the National Academy of Sciences, 107,
865 18634–18639, 2010.

866 Conway, J. R., Lex, A., and Gehlenborg, N.: UpSetR: an R package for the visualization of
867 intersecting sets and their properties, Bioinformatics, 2017.

868 Dai, C., Füllgrabe, A., Pfeuffer, J., Solovyeva, E. M., Deng, J., Moreno, P., Kamatchinathan, S.,
869 Kundu, D. J., George, N., and Fexova, S.: A proteomics sample metadata representation for
870 multiomics integration and big data analysis, Nature Communications, 12, 1–8, 2021.

871 Deutsch, E. W., Bandeira, N., Sharma, V., Perez-Riverol, Y., Carver, J. J., Kundu, D. J., García-
872 Seisdedos, D., Jarnuczak, A. F., Hewapathirana, S., Pullman, B. S., Wertz, J., Sun, Z., Kawano,
873 S., Okuda, S., Watanabe, Y., Hermjakob, H., MacLean, B., MacCoss, M. J., Zhu, Y., Ishihama,
874 Y., and Vizcaíno, J. A.: The ProteomeXchange consortium in 2020: enabling 'big data'
875 approaches in proteomics, Nucleic Acids Research, gkz984, https://doi.org/10.1093/nar/gkz984,
876 2019.

877 Falkowski, P.G., Fenchel, T. and Delong, E.F., 2008. The microbial engines that drive Earth's
878 biogeochemical cycles. science, 320(5879), 1034-1039.
879
880 Fuchsman, C. A., Palevsky, H. I., Widner, B., Duffy, M., Carlson, M. C., Neibauer, J. A.,
881 Mulholland, M. R., Keil, R. G., Devol, A. H., and Rocap, G.: Cyanobacteria and cyanophage
882 contributions to carbon and nitrogen cycling in an oligotrophic oxygen-deficient zone, The ISME
883 Journal, 13, 2714–2726, 2019.

884 Georges, A. A., El-Swais, H., Craig, S. E., Li, W. K., and Walsh, D. A.: Metaproteomic analysis
885 of a winter to spring succession in coastal northwest Atlantic Ocean microbial plankton, The
886 ISME journal, 8, 1301–1313, 2014.

887 Hawley, A. K., Brewer, H. M., Norbeck, A. D., Paša-Tolić, L., and Hallam, S. J.: Metaproteomics
888 reveals differential modes of metabolic coupling among ubiquitous oxygen minimum zone
889 microbes, Proceedings of the National Academy of Sciences, 111, 11395–11400, 2014.

890 Held, N. A., Sutherland, K. M., Webb, E. A., McIlvin, M. R., Cohen, N. R., Devaux, A. J.,
891 Hutchins, D. A., Waterbury, J. B., Hansel, C. M., and Saito, M. A.: Mechanisms and
892 heterogeneity of in situ mineral processing by the marine nitrogen fixer Trichodesmium revealed
893 by single-colony metaproteomics, ISME Communications, 1, 1–9, 2021.

894 Hulstaert, N., Shofstahl, J., Sachsenberg, T., Walzer, M., Barsnes, H., Martens, L. and Perez-
895 Riverol, Y., 2019. ThermoRawFileParser: modular, scalable, and cross-platform RAW file
896 conversion. *Journal of Proteome Research*, *19*(1), 537-542.
897
898 Hyatt, D., Chen, G.-L., LoCascio, P. F., Land, M. L., Larimer, F. W., and Hauser, L. J.: Prodigal:
899 prokaryotic gene recognition and translation initiation site identification, BMC bioinformatics, 11,
900 1–11, 2010.

901 Jagtap, P. D., Hoopmann, M. R., Neely, B. A., Harvey, A., Käll, L., Perez-Riverol, Y., Abajorga,
902 M. K., Thomas, J. A., Weintraub, S. T., and Palmblad, M.: The Association of Biomolecular
903 Resource FacilitiesProteome Informatics Research Group Study on Metaproteomics(iPRG-
904 2020), J Biomol Tech, 34, 3fc1f5fe.a058bad4, https://doi.org/10.7171/3fc1f5fe.a058bad4, 2023.

905 Joy-Warren, H. L., Alderkamp, A.-C., van Dijken, G. L., J Jabre, L., Bertrand, E. M., Baldonado,
906 E. N., Glickman, M. W., Lewis, K. M., Middag, R., and Seyitmuhammedov, K.: Springtime
907 phytoplankton responses to light and iron availability along the western Antarctic Peninsula,
908 Limnology and Oceanography, 67, 800–815, 2022.

909 Kanehisa, M., Sato, Y., and Morishima, K.: BlastKOALA and GhostKOALA: KEGG tools for
910 functional characterization of genome and metagenome sequences, Journal of molecular
911 biology, 428, 726–731, 2016.

912

913 Keller, A., Nesvizhskii, A.I., Kolker, E. and Aebersold, R., 2002. An explanation of the Peptide
914 Prophet algorithm developed. *Anal. Chem*, *74*(2002), 5383-5392.

915

916 Kim, S. and Pevzner, P.A., 2014. MS-GF+ makes progress towards a universal database
917 search tool for proteomics. *Nature Communications*, *5*(1), 5277.

918

919 Kiweler, M., Looso, M. and Graumann, J., 2019. MARMoSET–extracting publication-ready mass
920 spectrometry metadata from RAW files. *Molecular & Cellular Proteomics*, *18*(8), 1700-1702.

921

922 Kleiner, M., Thorson, E., Sharp, C. E., Dong, X., Liu, D., Li, C., and Strous, M.: Assessing
923 species biomass contributions in microbial communities via metaproteomics, Nature
924 Communications, 8, 1–14, 2017.

925 Kleiner, M., 2019. Metaproteomics: much more than measuring gene expression in microbial
926 communities. *Msystems*, *4*(3), 1128/msystems.00115-19.

927

928 Leary, D. H., Li, R. W., Hamdan, L. J., Hervey IV, W. J., Lebedev, N., Wang, Z., Deschamps, J.
929 R., Kusterbeck, A. W., and Vora, G. J.: Integrated metagenomic and metaproteomic analyses of
930 marine biofilm communities, Biofouling, 30, 1211–1223, 2014.

931 Malmstrom, R. R., Coe, A., Kettler, G. C., Martiny, A. C., Frias-Lopez, J., Zinser, E. R., and
932 Chisholm, S. W.: Temporal dynamics of Prochlorococcus ecotypes in the Atlantic and Pacific
933 oceans, The ISME journal, 4, 1252–1264, 2010.

934 McCain, J. S. P. and Bertrand, E. M.: Prediction and consequences of cofragmentation in
935 metaproteomics, Journal of proteome research, 18, 3555–3566, 2019.

936 McCain, J. S. P., Allen, A. E., and Bertrand, E. M.: Proteomic traits vary across taxa in a coastal
937 Antarctic phytoplankton bloom, The ISME journal, 16, 569–579, 2022.

938 McIlvin, M. R. and Saito, M. A.: Online Nanoflow Two-Dimension Comprehensive Active
939 Modulation Reversed Phase–Reversed Phase Liquid Chromatography High-Resolution Mass
940 Spectrometry for Metaproteomics of Environmental and Microbiome Samples, Journal of
941 proteome research, 20, 4589–4597, 2021.

942 Mikan, M. P., Harvey, H. R., Timmins-Schiffman, E., Riffle, M., May, D. H., Salter, I., Noble, W.
943 S., and Nunn, B. L.: Metaproteomics reveal that rapid perturbations in organic matter prioritize
944 functional restructuring over taxonomy in western Arctic Ocean microbiomes, The ISME journal,
945 14, 39–52, 2020.

946 Moore, E. K., Nunn, B. L., Goodlett, D. R., and Harvey, H. R.: Identifying and tracking proteins
947 through the marine water column: Insights into the inputs and preservation mechanisms of
948 protein in sediments, Geochimica et cosmochimica acta, 83, 324–359, 2012.

949

950 Moran, M.A., Kujawinski, E.B., Schroer, W.F., Amin, S.A., Bates, N.R., Bertrand, E.M.,
951 Braakman, R., Brown, C.T., Covert, M.W., Doney, S.C. and Dyhrman, S.T., 2022. Microbial
952 metabolites in the marine carbon cycle. *Nature microbiology*, 7(4), 508-523.

953

954 Morris, R. M., Nunn, B. L., Frazar, C., Goodlett, D. R., Ting, Y. S., and Rocap, G.: Comparative
955 metaproteomics reveals ocean-scale shifts in microbial nutrient utilization and energy
956 transduction, The ISME journal, 4, 673–685, 2010.

957 Mueller, R. S. and Pan, C.: Sample handling and mass spectrometry for microbial
958 metaproteomic analyses, in: Methods in Enzymology, vol. 531, Elsevier, 289–303, 2013.

959 Nesvizhskii, A.I., Keller, A., Kolker, E. and Aebersold, R., 2003. A statistical model for identifying
960 proteins by tandem mass spectrometry. *Analytical Chemistry*, 75(17), 4646-4658.

961

962 Piehowski, P. D., Petyuk, V. A., Orton, D. J., Xie, F., Moore, R. J., Ramirez-Restrepo, M., Engel,
963 A., Lieberman, A. P., Albin, R. L., and Camp, D. G.: Sources of technical variability in
964 quantitative LC–MS proteomics: human brain tissue sample analysis, Journal of proteome
965 research, 12, 2128–2137, 2013.

966 Pietilä, S., Suomi, T., and Elo, L. L.: Introducing untargeted data-independent acquisition for
967 metaproteomics of complex microbial samples, ISME COMMUN., 2, 51,
968 https://doi.org/10.1038/s43705-022-00137-0, 2022.

969 Ram, R. J., VerBerkmoes, N. C., Thelen, M. P., Tyson, G. W., Baker, B. J., Blake, R. C., Shah,
970 M., Hettich, R. L., and Banfield, J. F.: Community proteomics of a natural microbial biofilm,
971 Science, 308, 1915–1920, 2005.

972 Saito, M. A., McIlvin, M. R., Moran, D. M., Goepfert, T. J., DiTullio, G. R., Post, A. F., and
973 Lamborg, C. H.: Multiple nutrient stresses at intersecting Pacific Ocean biomes detected by
974 protein biomarkers, Science, 345, 1173–1177, 2014.

975 Saito, M. A., Dorsk, A., Post, A. F., McIlvin, M. R., Rappé, M. S., DiTullio, G. R., and Moran, D.
976 M.: Needles in the blue sea: Sub-species specificity in targeted protein biomarker analyses
977 within the vast oceanic microbial metaproteome, Proteomics, 15, 3521–3531, 2015.

978 Saito, M. A., Bertrand, E. M., Duffy, M. E., Gaylord, D. A., Held, N. A., Hervey IV, W. J., Hettich,
979 R. L., Jagtap, P. D., Janech, M. G., and Kinkade, D. B.: Progress and challenges in ocean
980 metaproteomics and proposed best practices for data sharing, Journal of proteome research,
981 18, 1461–1476, 2019.

982 Saito, M. A., McIlvin, M. R., Moran, D. M., Santoro, A. E., Dupont, C. L., Rafter, P. A., Saunders,
983 J. K., Kaul, D., Lamborg, C. H., and Westley, M.: Abundant nitrite-oxidizing metalloenzymes in
984 the mesopelagic zone of the tropical Pacific Ocean, Nature Geoscience, 13, 355–362, 2020.

985 Saunders, J. K., Gaylord, D. A., Held, N. A., Symmonds, N., Dupont, C. L., Shepherd, A.,
986 Kinkade, D. B., and Saito, M. A.: METATRYP v 2.0: Metaproteomic least common ancestor
987 analysis for taxonomic inference using specialized sequence assemblies—standalone software
988 and web servers for marine microorganisms and coronaviruses, Journal of proteome research,
989 19, 4718–4729, 2020.

990   Scanlan, D. J., Silman, N. J., Donald, K. M., Wilson, W. H., Carr, N. G., Joint, I., and Mann, N.
991   H.: An immunological approach to detect phosphate stress in populations and single cells of
992   photosynthetic picoplankton, Applied and environmental microbiology, 63, 2411–2420, 1997.

993   Schiebenhoefer, H., Van Den Bossche, T., Fuchs, S., Renard, B. Y., Muth, T., and Martens, L.:
994   Challenges and promise at the interface of metaproteomics and genomics: an overview of
995   recent progress in metaproteogenomic data analysis, Expert Review of Proteomics, 16, 375–
996   390, 2019.

997   Sørensen, T.: A method of establishing groups of equal amplitude in plant sociology based on
998   similarity of species and its application to analyses of the vegetation on Danish common.,
999   Kongelige Danske Videnskabernes Selskab, 5, 1–34, 1948.

1000 Sowell, S. M., Wilhelm, L. J., Norbeck, A. D., Lipton, M. S., Nicora, C. D., Barofsky, D. F.,
1001 Carlson, C. A., Smith, R. D., and Giovanonni, S. J.: Transport functions dominate the SAR11
1002 metaproteome at low-nutrient extremes in the Sargasso Sea, The ISME journal, 3, 93–105,
1003 2009.

1004 Stewart, H. I., Grinfeld, D., Giannakopulos, A., Petzoldt, J., Shanley, T., Garland, M., Denisov,
1005 E., Peterson, A. C., Damoc, E., Zeller, M., Arrey, T. N., Pashkova, A., Renuse, S., Hakimi, A.,
1006 Kühn, A., Biel, M., Kreutzmann, A., Hagedorn, B., Colonius, I., Schütz, A., Stefes, A., Dwivedi,
1007 A., Mourad, D., Hoek, M., Reitemeier, B., Cochems, P., Kholomeev, A., Ostermann, R., Quiring,
1008 G., Ochmann, M., Möhring, S., Wagner, A., Petker, A., Kanngiesser, S., Wiedemeyer, M.,
1009 Balschun, W., Hermanson, D., Zabrouskov, V., Makarov, A. A., and Hock, C.: Parallelized
1010 Acquisition of Orbitrap and Astral Analyzers Enables High-Throughput Quantitative Analysis,
1011 Anal. Chem., 95, 15656–15664, https://doi.org/10.1021/acs.analchem.3c02856, 2023.

1012 Tagliabue, A.: 'Oceans are hugely complex': modelling marine microbes is key to climate
1013 forecasts, Nature, 623, 250–252, https://doi.org/10.1038/d41586-023-03425-4, 2023.

1014 Timmins-Schiffman, E., May, D. H., Mikan, M., Riffle, M., Frazar, C., Harvey, H. R., Noble, W.
1015 S., and Nunn, B. L.: Critical decisions in metaproteomics: achieving high confidence protein
1016 annotations in a sea of unknowns, The ISME journal, 11, 309–314, 2017.

1017 Ustick, L. J., Larkin, A. A., Garcia, C. A., Garcia, N. S., Brock, M. L., Lee, J. A., Wiseman, N. A.,
1018 Moore, J. K., and Martiny, A. C.: Metagenomic analysis reveals global-scale patterns of ocean
1019 nutrient limitation, Science, 372, 287–291, 2021.

1020 Van Den Bossche, T., Kunath, B. J., Schallert, K., Schäpe, S. S., Abraham, P. E., Armengaud,
1021 J., Arntzen, M. Ø., Bassignani, A., Benndorf, D., and Fuchs, S.: Critical Assessment of
1022 MetaProteome Investigation (CAMPI): a multi-laboratory comparison of established workflows,
1023 Nature communications, 12, 1–15, 2021.

1024 Virtanen, P., Gommers, R., Oliphant, T. E., Haberland, M., Reddy, T., Cournapeau, D.,
1025 Burovski, E., Peterson, P., Weckesser, W., and Bright, J.: SciPy 1.0: fundamental algorithms for
1026 scientific computing in Python, Nature methods, 17, 261–272, 2020.

1027 Waskom, M. L.: Seaborn: statistical data visualization, Journal of Open Source Software, 6,
1028 3021, 2021.

1029 Williams, T. J., Long, E., Evans, F., DeMaere, M. Z., Lauro, F. M., Raftery, M. J., Ducklow, H.,
1030 Grzymski, J. J., Murray, A. E., and Cavicchioli, R.: A metaproteomic assessment of winter and
1031 summer bacterioplankton from Antarctic Peninsula coastal surface waters, The ISME journal, 6,
1032 1883–1900, 2012.

1033 Wilmes, P. and Bond, P. L.: Metaproteomics: studying functional gene expression in microbial
1034 ecosystems, Trends in microbiology, 14, 92–97, 2006.

1035 Wilmes, P., Andersson, A. F., Lefsrud, M. G., Wexler, M., Shah, M., Zhang, B., Hettich, R. L.,
1036 Bond, P. L., VerBerkmoes, N. C., and Banfield, J. F.: Community proteogenomics highlights
1037 microbial strain-variant protein expression within activated sludge performing enhanced
1038 biological phosphorus removal, The ISME journal, 2, 853–864, 2008.

1039 Worden, A.Z., Follows, M.J., Giovannoni, S.J., Wilken, S., Zimmerman, A.E. and Keeling, P.J.,
1040 2015. Rethinking the marine carbon cycle: factoring in the multifarious lifestyles of
1041 microbes. *Science*, *347*(6223), 1257594.

1042

1043 Wu, M., McCain, J. S. P., Rowland, E., Middag, R., Sandgren, M., Allen, A. E., and Bertrand, E.
1044 M.: Manganese and iron deficiency in Southern Ocean Phaeocystis antarctica populations
1045 revealed through taxon-specific protein indicators, Nature communications, 10, 1–10, 2019.

1046
1047

1048 **Figure Captions**

1049 **Figure 1.** Ocean metaproteomics intercomparison experimental design and sample collection.

1050 a) The laboratory component (left) consisted of collection of field samples, 1-dimensional (1D)

1051 chromatographic separation followed by data dependent analysis (DDA) uniformly employing

1052 orbitrap mass spectrometers analyses by participating laboratories and submission of raw and

1053 processed data. The bioinformatic (right) component consisted of distribution of two 1D-DDA

1054 files, peptide-to-spectrum matching (PSMs), and submission and compilation of results. b) Size-

1055 fractionated sample collection on 3.0 μm pore-size filter followed by a 0.2 μm pore-size Supor

1056 filter, and the 0.2–3.0 μm size fraction was used for the intercomparison study. c) Two horizontal

1057 *in-situ* McLane pumps were bracketed together with two Mini-MULVS filter head units each and

1058 deployment on synthetic line. d) The four 142 mm filters were sliced into eighths (inset) and two

1059 slices were distributed to each participating laboratory.

1060

1061 **Figure 2.** Shared peptides and proteins between laboratory groups using laboratory

1062 submissions processed through a single bioinformatics re-analysis pipeline. a) Total number of

1063 discovered unique peptides varied by more than three-fold among seven laboratory groups

1064 (horizontal bars) due to varying extraction and analytical schemes (FDR 0.1%). The number of

1065 intersections between datasets across all seven datasets was 1395 (fourth blue bar from left),

1066 and various sets of intersections of peptides were observed amongst the data. b) Total number

1067 of discovered proteins (FDR < 1%) varied more than four-fold from 1586 to 6221 among labs

1068 (horizontal bars). Intersections between datasets across all seven laboratories was 1056, with

1069 various sets of intersections of proteins observed, similar to the peptides. c) 7-way Venn

1070 diagrams of shared unique peptides between laboratories showed 1056 shared peptides

1071 between the 7 laboratories. d) 3-way Venn diagrams showed 2398, 2304, and 3016 shared

1072 unique peptides between laboratories.

1073

1074 **Figure 3.** Comparison of unique peptides and discovered proteins. Comparison as total protein

1075 identifications and protein groups from the single pipeline re-analysis based on submissions

1076 from 9 laboratories. Increasing sample depth is linear with mapping to proteins, (R^2 of 0.97 and

1077 0.98 for total protein IDs and protein groups, respectively, with slopes of 0.37 and 33) implying

1078 that additional peptide discovery leads to proportionally more protein discovery, and that protein

1079 discovery has not yet begun to saturate with more peptides mapping to each protein. Because

1080 simple 1D analyses were stipulated in the intercomparison experimental design, peptide and

1081 protein discovery was correspondingly limited in depth.

1082

1083 **Figure 4.** Quantitative comparison of intercomparison results. a) Pairwise comparisons of

1084 quantitative abundance across six laboratories in units of spectral counts (comparisons with

1085 itself show unison diagonals). b) R^2 values from pairwise linear regressions. d) Total proteins

1086 identified in each laboratory. d) Average of each laboratory's R^2 values from pairwise regression

1087 with the other six laboratories (error bars are standard deviation). In all cases average R^2 values

1088 are higher than 0.5. e) Occurrences of R^2 values in pairwise comparisons spanning 0.4 to 0.9.

1089 Potential causes of this range are outlined in the Discussion section.

1090

1091 **Figure 5.** Taxonomic and functional analysis of metaproteomic intercomparison. a) Percent

1092 spectral counts by taxonomy was similar across laboratories and technical replicates within

1093 laboratories. The sample was dominated by cyanobacteria and alphaproteobacteria,

1094 corresponding primarily to *Prochlorococcus* and *Pelagibacter*, respectively. b) Percent spectral

1095 counts per Kegg Ontology group showed the functional diversity of the sample.

1096

1097 **Figure 6.** Quantitative Sørensen similarity analysis. Analysis of top 1000 proteins (~75% of all

1098 proteins) showed 70–80% similarity between most laboratory groups. Technical triplicates for

1099   each laboratory group are shown.

1100

1101   **Figure 7.** Intercomparison of bioinformatic pipelines among laboratories. Unique peptide

1102   identifications for sample Ocean 8 from 120m depth (a) and Ocean 11 from 20m depth (b), both

1103   from the North Atlantic Ocean (Table S3), using a variety of pipelines and PSM algorithms.

1104

1105   **Figure 8.** Variability in discovered proteins between laboratories occurs in lower abundance

1106   proteins. Top 7 panels: Abundance of proteins as percentage of total protein spectral counts

1107   within each laboratory (y-axis is percentage), with proteins on the x-axis shown by ranked

1108   abundance as the sum of spectral counts across all laboratories. Almost all proteins fall below

1109   1% of spectral counts within the sample, and deeper proteomes have lower percentages due to

1110   sharing of percent spectral counts across more discovered proteins. Bottom panel: Shared

1111   proteins were found early within the long-tail of discovered proteins: the 1056 proteins shared

1112   between all laboratory groups are almost all found to the left side indicating their higher

1113   abundance in all seven datasets. Scale is binary in the seventh panel indicating presence in 7

1114   labs or not.

1115

1116

1117   Figure 1.

1118

1119

1120
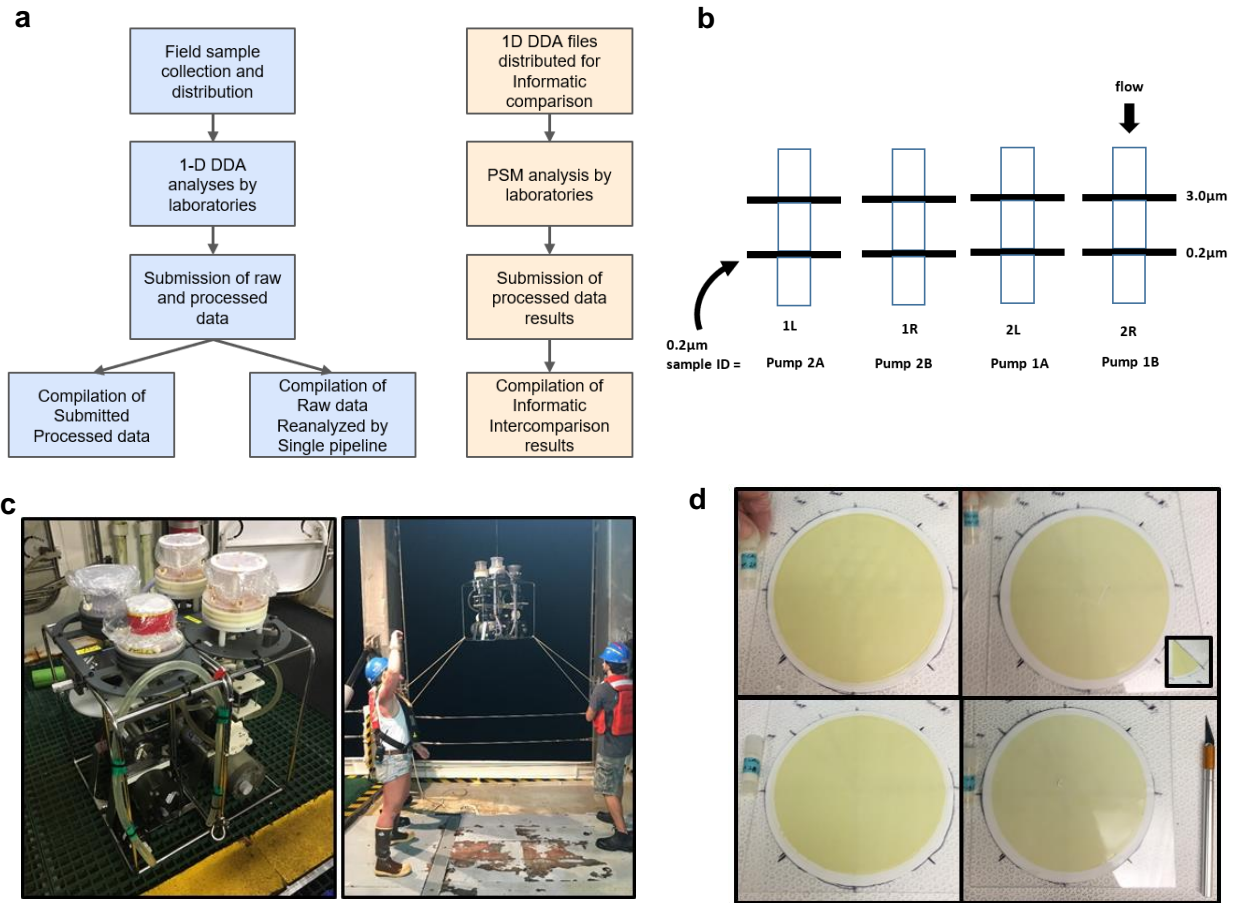
1121   Figure 2.

1122
a

1123

c

1124

1125

d
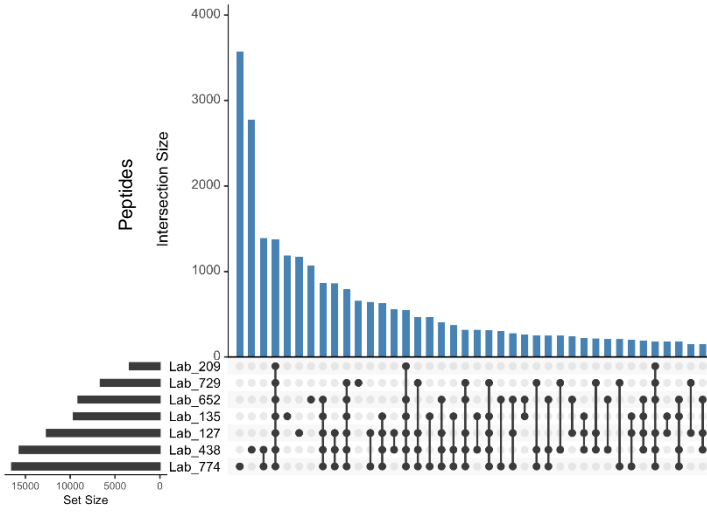
1126
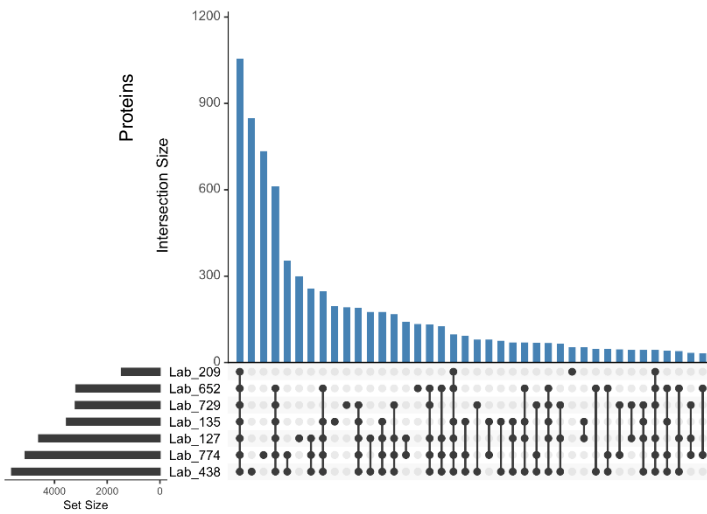
1127

1132

1133

1134
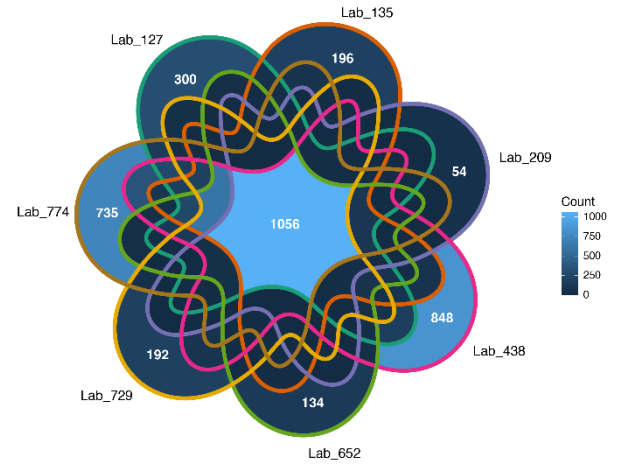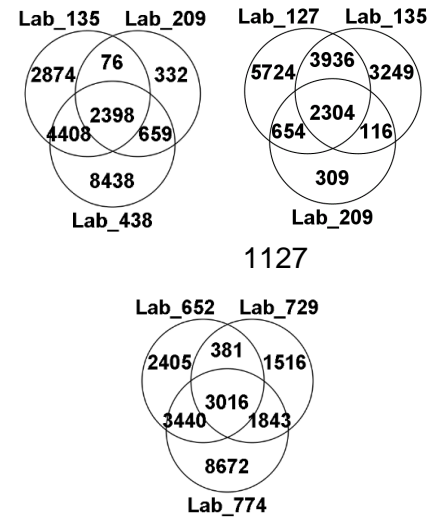
1135   Figure 3

1136

1137

1138

1139

1140

1141

1142

1143
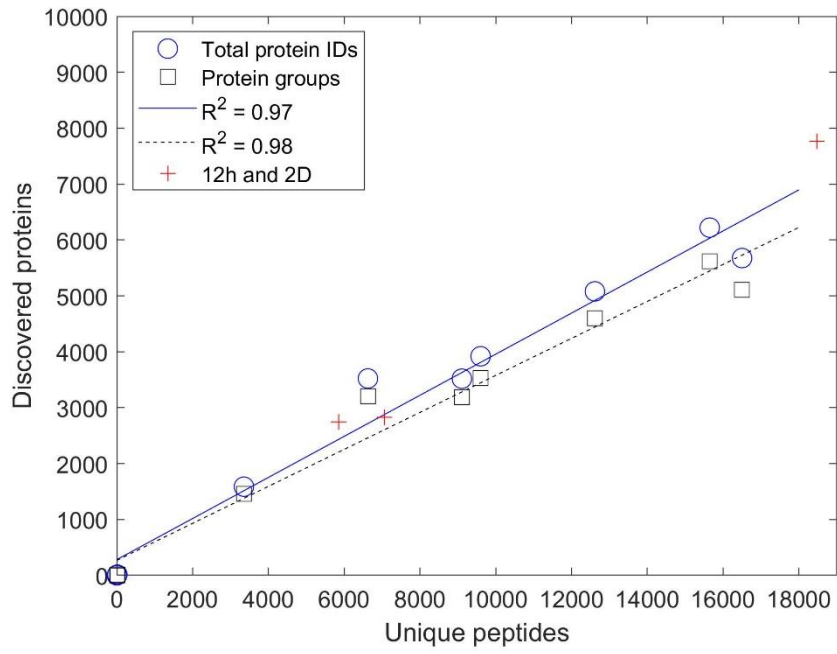
1144   Figure 4.

1145
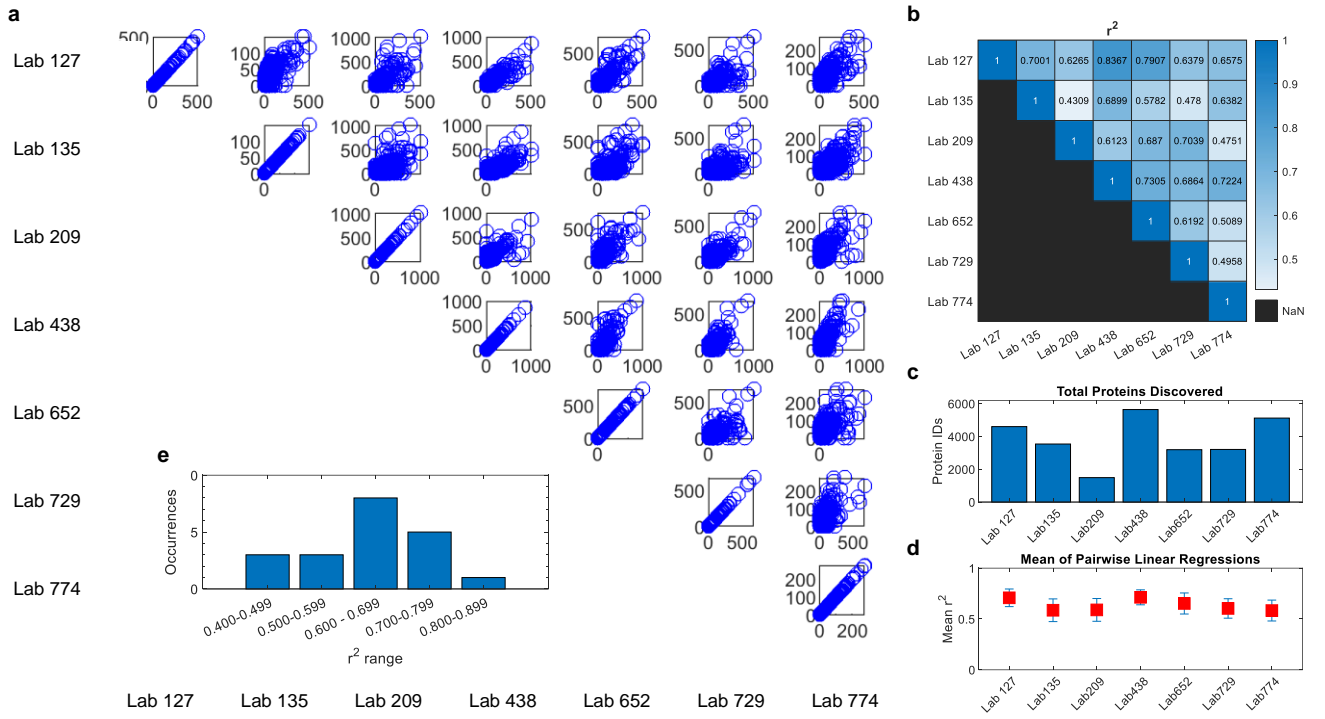
1146

1147

1148

1149   Figure 5.

1150

1151

1152

1153

a

b
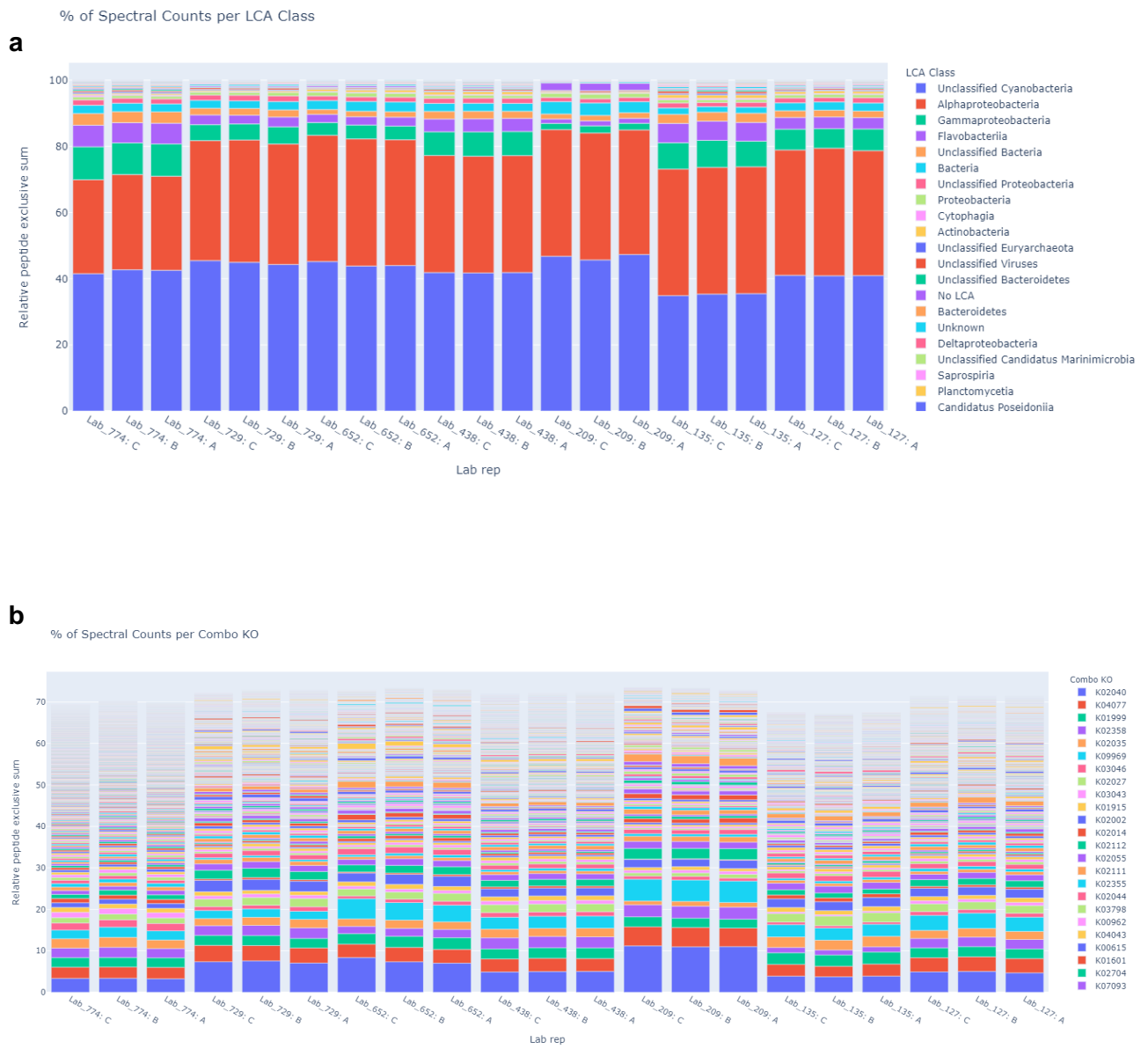
1162   Figure 6.

1163
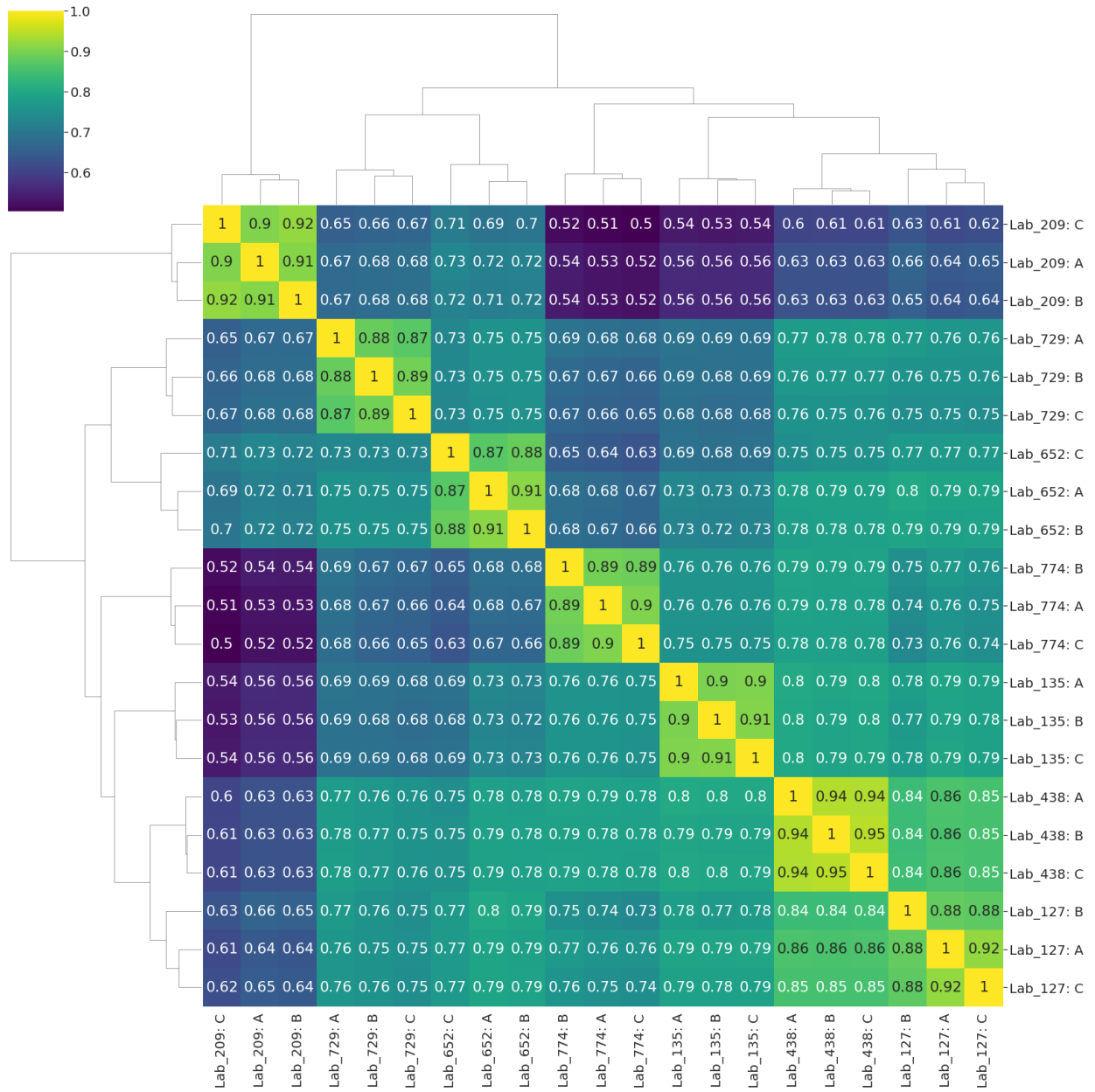
1164

1165

1166

1167

1168

1169

1170   Figure 7.

1171

1172

1173

a   **b**
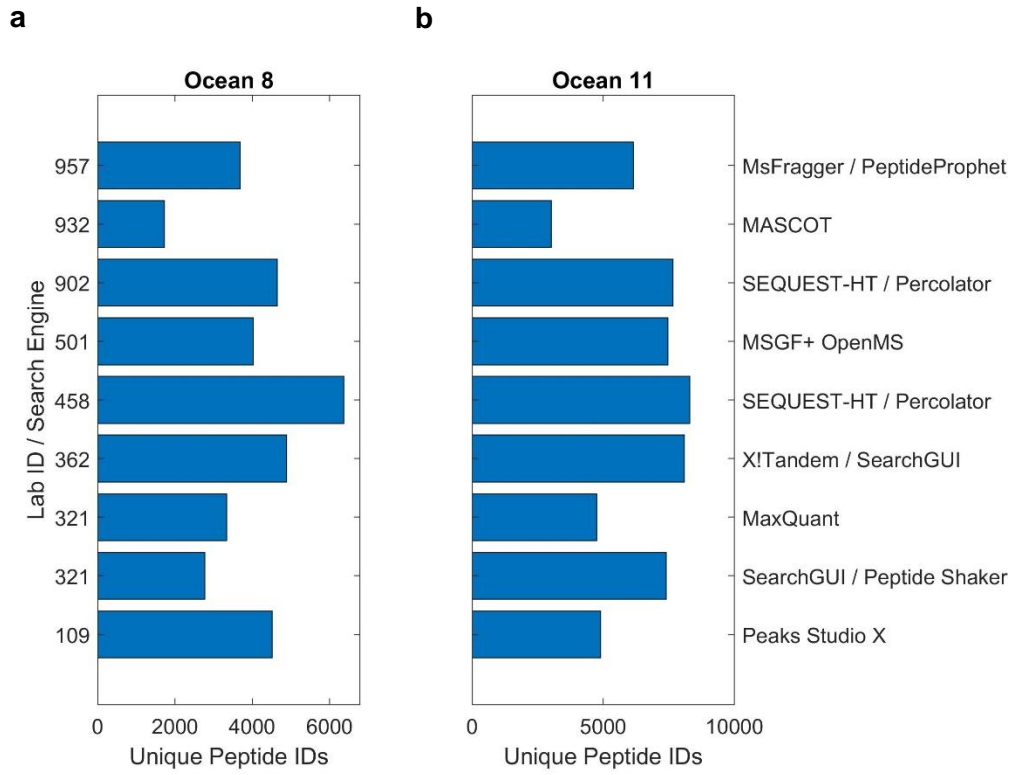
1174

1175

1176   Figure 8.

1177